Standard Model anatomy of WIMP dark matter direct detection. II. QCD analysis and hadronic matrix elements

Richard J. Hill and Mikhail P. Solon

Phys. Rev. D **91**, 043505 — Published 5 February 2015

DOI: 10.1103/PhysRevD.91.043505

EFI Preprint 14-25

Standard Model anatomy of WIMP dark matter direct detection II: QCD analysis and hadronic matrix elements

Richard J. Hill[1] and Mikhail P. Solon[1,2]

[1] *Enrico Fermi Institute and Department of Physics*
The University of Chicago, Chicago, Illinois, 60637, USA

[2] *Berkeley Center for Theoretical Physics, Department of Physics*
and Theoretical Physics Group, Lawrence Berkeley National Laboratory
University of California, Berkeley, CA 94270, USA

Abstract

Models of Weakly Interacting Massive Particles (WIMPs) specified at the electroweak scale are systematically matched to effective theories at hadronic scales where WIMP-nucleus scattering observables are evaluated. Anomalous dimensions and heavy quark threshold matching conditions are computed for the complete basis of lowest-dimension effective operators involving quarks and gluons. The resulting QCD renormalization group evolution equations are solved. The status of relevant hadronic matrix elements is reviewed and phenomenological illustrations are given, including details for the computation of the universal limit of nucleon scattering with heavy $SU(2)_W \times U(1)_Y$ charged WIMPs. Several cases of previously underestimated hadronic uncertainties are isolated. The results connect arbitrary models specified at the electroweak scale to a basis of $n_f = 3$ flavor QCD operators. The complete basis of operators and Lorentz invariance constraints through order v^2/c^2 in the nonrelativistic nucleon effective theory are derived.

1 Introduction

In the search for Weakly Interacting Massive Particles (WIMPs), experiments in the present decade and beyond will explore a broad range of processes [1], such as dark matter (DM) production at colliders, DM annihilation at the galactic center and DM scattering from nuclear targets. Given the multitude of WIMP candidates and search strategies, it is imperative to develop theoretical formalism to delineate the possible interactions of DM with known particles, making clear which uncertainties are inherently model dependent and which can, at least in principle, be improved by further Standard Model (SM) analysis.

Particularly in the case of direct detection via nuclear scattering, determining the relation between an underlying particle physics model and the experimental observable (i.e., scattering cross section) demands analysis at multiple energy scales involving both perturbative and nonperturbative QCD. Relating physics at (and above) the weak scale to an effective theory in which hadronic observables are evaluated is a problem that has received significant attention in other arenas, such as flavor transitions involving heavy mesons [2] and electric dipole moment searches [3]. The analogous problem in dark matter direct detection contains a unique set of challenges whose study is the focus of the preceding [4] and present paper. In [4] we described the steps involved in matching an ultraviolet completion DM model, consisting of some number of SM gauge multiplets, onto an effective theory renormalized at the weak scale. Here we develop the framework for the systematic treatment of QCD effects when passing from a theory renormalized at the weak scale to a low-energy theory of quarks and gluons. We also identify pieces of the framework whose further development significantly impacts our knowledge of WIMP-nucleus scattering cross sections, including heavy quark decoupling relations in perturbative QCD, and nonperturbative scalar quark matrix elements of the nucleon in $n_f = 3$ or $n_f = 4$ flavor QCD. The results of this analysis can be used as the basis for detailed nuclear modeling. To this end we derive the nucleon-level effective theory and matching conditions through two-derivative order in the one-nucleon sector.

While the theoretical formalism is general, for the purposes of illustration we focus our phenomenological illustrations on the analysis of heavy $SU(2)_W \times U(1)_Y$ charged WIMPs. We do so for three reasons. Firstly, this scenario is highly predictive: in the limit of large WIMP mass, the WIMP-nucleon scattering amplitude is completely determined solely by SM parameters; secondly, this regime provides an important illustration of QCD effects, since generic cancellations between subamplitudes enhance sensitivity to subleading corrections; and thirdly, the hitherto absence of significant deviations between observations and SM predictions at the Large Hadron Collider and elsewhere may actually indicate a new physics scale lying somewhat above m_W, $m_Z \sim 100\,\mathrm{GeV}$.

The unknown particle nature of dark matter is the source of great intrigue but also complicates any analysis wishing to draw unambiguous conclusions. The separation of energy scales, formalized by a sequence of effective theories, provides several choices for starting point when constraining potential WIMP interactions with SM fields, or in relating constraints or potential signals between observational methods. Each effective theory takes as input matching conditions computed in a higher scale theory; alternatively, giving up the connection to the high scale theory, one may start at any point in the sequence by taking effective operator coefficients as free parameters to be constrained by experiment.

At the highest scales, a UV complete model may be specified [5, 6, 7], but may involve many poorly constrained parameters with degenerate effects on low energy observables. Restriction to a small number of postulated fields [8, 9, 10, 11, 12, 13, 14], reduces the parameter number, but typically without justification for choice of field content. A sparse distribution of pure gauge states (measured in units of m_W) becomes generic when masses of particles beyond the SM (BSM) become large

compared to m_W. Here the heavy WIMP expansion maintains theoretical control in the absence of a specified UV completion and dramatically simplifies loop integral computations that become numerically dominant in this regime [15, 16, 4]. In the case of an assumed large mass scale for BSM particles mediating interactions with the SM, a basis of contact interactions can be investigated [17, 18], although the connection between such contact interactions and UV completions may be unclear. As illustrated below in Section 6.1, care should also be taken to account for renormalization scale and scheme dependence when relating high scale constraints to low scale observables. The effects of renormalization group running in theories above the weak scale have been investigated in [19, 20].

Under the assumption that BSM particles (except perhaps the DM itself) have mass at or above the weak scale, the remaining analysis is independent of which of the above approaches is taken to physics above the weak scale. The focus of the present paper is on the task of relating the resulting effective theory specified at the weak scale to the effective theory defined at low energy where hadronic matrix elements are evaluated. This $n_f = 3$ flavor QCD theory is the natural handoff point from particle to nuclear physics. Here again, there are several choices for the starting point of a nuclear physics effective theory analysis. To the extent that nuclear matrix elements are determined by single nucleon matrix elements, an alternative would be to take the coefficients of single-nucleon operators as unknowns to be constrained by direct detection observables [21, 22, 23, 24], generalizing the canonical spin-independent and spin-dependent DM-nucleon interactions, cf. (79) below, commonly considered in the presentation of DM direct detection limits [25, 1]. As discussed below in Section 5.2.1, when including v^2/c^2 effects it is important to properly enforce Lorentz versus Galilean invariance in the effective Lagrangian. To the extent that multi-nucleon effects are relevant, the complete nuclear response cannot be derived from information contained solely in the single nucleon matching, requiring an extension of the effective theory to include such effects and/or additional information from quark-level matching [26]. A heavy particle effective theory may be constructed for an entire nucleus [27] but requires further analysis in order to directly compare experiments using different nuclei [28].[1]

The remainder of the paper is structured as follows. In Section 2 we discuss the construction of complete operator bases for DM-SM interactions after integrating out weak scale particles. We present leading order weak scale matching conditions onto the lowest dimension effective theory operators for an illustrative UV completion involving gauge-singlet DM (the case of $SU(2)_W \times U(1)_Y$ charged dark matter was considered in [4]). In Section 3 we compute the relevant operator renormalization factors and anomalous dimensions. This section also presents the renormalization group evolution of effective operators and coefficients, and matching conditions at heavy quark thresholds. Section 4 reviews the relevant hadronic matrix elements and Section 5 describes the associated nucleon-level effective theory. Section 6 gives phenomenological illustrations of QCD effects in DM direct detection. For example, the results for renormalization factors in Sec. 3 are combined with the computation in [4] to obtain renormalized ($\overline{\rm MS}$) matching coefficients at the weak scale for electroweak-charged self-conjugate heavy WIMPs. Section 7 concludes with a summary and outlook. Appendices provide details of renormalization constants, and higher order nucleon matrix elements discussed in the main text.

[1] Other recent studies of general WIMP-nucleon interactions include [29, 30, 31, 32]. For a review including further references to early work, see [5].

2 Effective theory below the electroweak scale

The tabulation of operators at a given mass dimension involving SM fields and a finite collection of DM fields of given SM quantum numbers is a straightforward task, but requires some care to ensure a complete basis while avoiding redundant operators. We construct operator bases appropriate to energies below the weak scale, enforcing $SU(3)_c \times U(1)_{\rm e.m.} \times U(1)_{\rm DM}$ or $SU(3)_c \times U(1)_{\rm e.m.} \times Z_2$ invariance, assuming a $U(1)_{\rm DM}$ or Z_2 symmetry to stabilize the DM particle. The massive electroweak gauge bosons, $W^\pm, Z^0$, the top quark, t, and the physical Higgs field, h, are integrated out, and we consider higher dimension operators suppressed by the weak scale, for definiteness taken to be m_W. We focus on two cases: firstly, the case $M \gtrsim m_W$ for SM interactions with the (assumed electrically neutral) lightest state of a BSM sector; and secondly, the case $M \ll m_W$ for SM interactions with a gauge singlet scalar or fermion. These cases cover a large space of models, and illustrate principles in any more general analysis.

2.1 Standard Model building blocks

For the SM degrees of freedom, we focus on the quark and gluon fields of $n_f = 5$ flavor QCD, and consider the photon field only in the case of dimension five electric and magnetic dipole operators, i.e., when operators containing the photon are of lower dimension than quark and gluon operators. Operators with leptons may be constructed similarly to quark operators. The flavor diagonal, Hermitian, gauge-invariant SM building blocks through dimension four are

$$F^{\mu\nu}\,, \quad \bar{q}\big[\gamma^\mu\,, \gamma^\mu\gamma_5\big]\big[1\,, iD^\rho_-\big]q\,, \quad G^A_{\mu\nu}G^A_{\rho\sigma}\,. \tag{1}$$

We will perform Fierz rearrangements to the basis without spinor contractions between SM and DM fields, hence only free vector indices appear in (1). Collected within square brackets, [ ], are the different structures that may be applied to the same field bilinear. Total derivatives of building blocks are not listed above but must be considered in the construction of the effective lagrangian. We use the shorthand $D^\mu_\pm \equiv D^\mu \pm \overleftarrow{D}^\mu$, where $D_\mu = \partial_\mu - igA^A_\mu T^A - ieQA_\mu$ is the $SU(3)_c \times U(1)_{e.m.}$ covariant derivative and $\overleftarrow{D}_\mu = \overleftarrow{\partial}_\mu + igA^A_\mu T^A + ieQA_\mu$ with $\overleftarrow{\partial}$ denoting a derivative acting to the left. Here Q denotes the electric charge in units of the proton electric charge e.

In writing (1) we have considered only quark flavor diagonal operators and imposed global chiral symmetries $q_{L,R} \to e^{i\epsilon_{L,R}} q_{L,R}$ when quark masses vanish. These constraints can be formally justified by restricting to ultraviolet completions for which a $U(3)_L \times U(3)^u_R \times U(3)^d_R$ symmetry ("minimal flavor violation") can be defined in the electroweak-symmetric theory. Additional operators through dimension four consistent with these requirements are

$$m_q \bar{q}\big[1\,, i\gamma_5\,, \sigma^{\mu\nu}\big]q\,. \tag{2}$$

However Lagrangian interactions containing (2) can be shown to be redundant by field redefinitions, leaving (1) as a complete basis of independent SM operators. It is straightforward to extend the building blocks in (1) to consider more general flavor structure.

2.2 Dark matter building blocks

For the dark sector, we focus on operators involving the lightest $SU(3)_c \times U(1)_{\rm e.m.}$-singlet WIMP state. We collect in the first two columns of Table 1 the lowest dimension Hermitian, gauge-invariant DM bilinears for relativistic scalar and fermion fields, denoted respectively by a complex valued ϕ

d	Fermion	d	Scalar	d	Heavy particle
3	$\bar{\psi}\big[1\,,\ i\gamma_5\,,\ \gamma^\mu\gamma_5\,,\ \{\gamma^\mu\,,\ \sigma^{\mu\nu}\}\big]\psi$	2	$\lvert\phi\rvert^2$	3	$\bar{\chi}_v\big[1\,,\ \{\sigma_\perp^{\mu\nu}\}\big]\chi_v$
4	$\bar{\psi}\big[\{1\,,\ i\gamma_5\,,\ \gamma^\mu\gamma_5\}\,,\ \gamma^\mu\,,\ \sigma^{\mu\nu}\big]i\partial_-^\rho\psi$	3	$\{\phi^* i\partial_-^\mu\phi\}$	4	$\bar{\chi}_v\big[\{1\}\,,\ \sigma_\perp^{\mu\nu}\big]i\partial_{\perp-}^\rho\chi_v$

Table 1: Gauge-invariant DM operator building blocks of indicated dimension for a relativistic fermion and scalar, and a heavy-particle fermion. For the relativistic case, building blocks within curly brackets, { }, vanish for self-conjugate fields such as a Majorana fermion or a real scalar. For the heavy-particle case, building blocks within curly brackets, { }, are odd under the parity in Eq. (3). The list for a heavy-particle scalar (of mass dimension 3/2) is obtained by omitting building blocks with the spin structure $\sigma_\perp^{\mu\nu}$ above.

and a four-component spinor ψ. We consider both the case where there is a conserved global $U(1)_{\rm DM}$ DM particle number, i.e., a Dirac fermion or complex scalar, and the case where the DM particle is self-conjugate and odd under an exact Z_2 symmetry, i.e., a Majorana fermion ($\psi = \psi^c$) or a real scalar ($\phi = \phi^*$). As for the SM building blocks, we ignore total derivatives of DM bilinears, which must be considered when constructing lagrangian interactions.

In the regime where the DM has mass comparable to or heavier than the electroweak scale particles, $M \gtrsim m_W$, the scale separation $M \gg m_b$ allows us to employ the heavy-particle building blocks listed in the final column of Table 1. We list the building blocks appropriate for a spin 1/2 or spin 0 heavy particle; effective theories for higher-spin particles may be similarly constructed. Lorentz transformations of the heavy particle field are governed by the little group for massive particles defined by the time-like unit vector v^μ. A heavy fermion has two degrees of freedom which may be embedded in a Dirac spinor, χ_v, with constraint $\not{v}\,\chi_v = \chi_v$ (see, e.g., Ref. [33] and Sec. 2 of Ref. [4] for more details). In writing the heavy-particle building blocks in Table 1 we assume field redefinitions that eliminate operators with timelike derivatives $v\cdot D$ acting on χ_v, and hence only perpendicular components of derivatives, $\partial_\perp^\mu$, appear. In a standard notation we define spacelike (with respect to the timelike unit vector v^μ) "perpendicular" components using $g_\perp^{\mu\nu} \equiv g^{\mu\nu} - v^\mu v^\nu$. In particular, we have $\partial_\perp^\mu \equiv \partial_\alpha g_\perp^{\alpha\mu} = \partial^\mu - v^\mu v\cdot\partial$ and $\sigma_\perp^{\mu\nu} \equiv \sigma_{\alpha\beta} g_\perp^{\alpha\mu} g_\perp^{\beta\nu}$.

For lagrangians containing heavy fields describing self-conjugate particles such as Majorana fermions or real scalars, we may furthermore impose invariance under the self-conjugate parity, enforced formally by the simultaneous operations [34, 15][2]

$$v^\mu \to -v^\mu\,, \quad \chi_v \to \chi_v^c = \mathcal{C}\chi_v^*\,. \tag{3}$$

Equivalently we may impose CPT invariance, applying the usual CPT transformations for relativistic fields, but employing a modified version of CPT for the heavy-particle, under which [3]

$$C:\chi(t,\boldsymbol{x})\to\xi\,\chi(t,\boldsymbol{x})\,,\quad P:\chi(t,\boldsymbol{x})\to\eta\,\chi(t,-\boldsymbol{x})\,,\quad T:\chi(t,\boldsymbol{x})\to\zeta\,S\,\chi(-t,\boldsymbol{x})\,, \tag{4}$$

where $S = i\sigma_2$ for fermions and $S = 1$ for scalars [33]. In this formulation of the self-conjugate parity, the action of discrete symmetries transforms fields, but leaves the reference vector v^μ unchanged. Hence, it may be readily employed even when the reference vector is fixed, e.g., to $v^\mu = (1,\mathbf{0})$ in the rest frame of the heavy particle.

[2] Here $\mathcal{C}$ is the charge conjugation matrix acting on the spinor index of χ_v. It is symmetric and unitary and satisfies $\mathcal{C}^\dagger\gamma_\mu\mathcal{C} = -\gamma_\mu^*$. For the extension to arbitrary spin see Ref. [33].

[3] The phases ξ, η and ζ under C, P and T do not affect scattering observables.

2.3 Operator basis

Upon combining the SM building blocks in (1) with the DM building blocks in Table 1, and performing field redefinitions to eliminate redundant operators, we obtain the effective lagrangian for DM interactions below the weak scale.

For the relativistic scalar case we have the following interactions,

$$\mathcal{L}_{\phi,\rm SM} = \sum_{q=u,d,s,c,b} \left\{ \frac{c_{\phi 1,q}}{m_W^2}|\phi|^2 m_q \bar{q}q + \frac{c_{\phi 2,q}}{m_W^2}|\phi|^2 m_q \bar{q}i\gamma_5 q + \frac{c_{\phi 3,q}}{m_W^2}\phi^* i\partial_-^\mu \phi \bar{q}\gamma_\mu q \right.$$
$$\left. + \frac{c_{\phi 4,q}}{m_W^2}\phi^* i\partial_-^\mu \phi \bar{q}\gamma_\mu\gamma_5 q \right\} + \frac{c_{\phi 5}}{m_W^2}|\phi|^2 G^A_{\alpha\beta}G^{A\alpha\beta} + \frac{c_{\phi 6}}{m_W^2}|\phi|^2 G^A_{\alpha\beta}\tilde{G}^{A\alpha\beta} + \dots . \tag{5}$$

For antisymmetric tensors we define the shorthand notation $\tilde{T}^{\mu\nu} = \epsilon^{\mu\nu\rho\sigma}T_{\rho\sigma}/2$ (we use the convention $\epsilon^{0123} = +1$). The ellipsis in (5) denotes operators of dimension six and higher involving the photon, and operators of dimension seven and higher involving quarks and gluons. For a real scalar the coefficients $c_{\phi n}$ vanish for $n = 3, 4$.

For the relativistic fermion case we have the following interactions,

$$\mathcal{L}_{\psi,\rm SM} = \frac{c_{\psi 1}}{m_W}\bar{\psi}\sigma^{\mu\nu}\psi F_{\mu\nu} + \frac{c_{\psi 2}}{m_W}\bar{\psi}\sigma^{\mu\nu}\psi \tilde{F}_{\mu\nu} + \sum_{q=u,d,s,c,b}\left\{ \frac{c_{\psi 3,q}}{m_W^2}\bar{\psi}\gamma^\mu\gamma_5\psi\bar{q}\gamma_\mu q + \frac{c_{\psi 4,q}}{m_W^2}\bar{\psi}\gamma^\mu\gamma_5\psi\bar{q}\gamma_\mu\gamma_5 q \right.$$
$$+ \frac{c_{\psi 5,q}}{m_W^2}\bar{\psi}\gamma^\mu\psi\bar{q}\gamma_\mu q + \frac{c_{\psi 6,q}}{m_W^2}\bar{\psi}\gamma^\mu\psi\bar{q}\gamma_\mu\gamma_5 q + \frac{c_{\psi 7,q}}{m_W^3}\bar{\psi}\psi m_q\bar{q}q + \frac{c_{\psi 8,q}}{m_W^3}\bar{\psi}i\gamma_5\psi m_q\bar{q}q$$
$$+ \frac{c_{\psi 9,q}}{m_W^3}\bar{\psi}\psi m_q\bar{q}i\gamma_5 q + \frac{c_{\psi 10,q}}{m_W^3}\bar{\psi}i\gamma_5\psi m_q\bar{q}i\gamma_5 q + \frac{c_{\psi 11,q}}{m_W^3}\bar{\psi}i\partial_-^\mu\psi\bar{q}\gamma_\mu q$$
$$+ \frac{c_{\psi 12,q}}{m_W^3}\bar{\psi}\gamma_5\partial_-^\mu\psi\bar{q}\gamma_\mu q + \frac{c_{\psi 13,q}}{m_W^3}\bar{\psi}i\partial_-^\mu\psi\bar{q}\gamma_\mu\gamma_5 q + \frac{c_{\psi 14,q}}{m_W^3}\bar{\psi}\gamma_5\partial_-^\mu\psi\bar{q}\gamma_\mu\gamma_5 q$$
$$\left. + \frac{c_{\psi 15,q}}{m_W^3}\bar{\psi}\sigma_{\mu\nu}\psi m_q\bar{q}\sigma^{\mu\nu}q + \frac{c_{\psi 16,q}}{m_W^3}\epsilon_{\mu\nu\rho\sigma}\bar{\psi}\sigma^{\mu\nu}\psi m_q\bar{q}\sigma^{\rho\sigma}q \right\} + \frac{c_{\psi 17}}{m_W^3}\bar{\psi}\psi G^A_{\alpha\beta}G^{A\alpha\beta}$$
$$+ \frac{c_{\psi 18}}{m_W^3}\bar{\psi}i\gamma_5\psi G^A_{\alpha\beta}G^{A\alpha\beta} + \frac{c_{\psi 19}}{m_W^3}\bar{\psi}\psi G^A_{\alpha\beta}\tilde{G}^{A\alpha\beta} + \frac{c_{\psi 20}}{m_W^3}\bar{\psi}i\gamma_5\psi G^A_{\alpha\beta}\tilde{G}^{A\alpha\beta} + \dots , \tag{6}$$

where the ellipsis denotes operators of dimension six and higher involving the photon, and operators of dimension eight and higher involving quarks and gluons. For a Majorana fermion the coefficients $c_{\psi n}$ with $n = 1, 2, 5, 6, 11, 12, 13, 14, 15, 16$ vanish, leaving ten types of operators through dimension seven as considered in Ref. [17].

For the case of DM with mass $M \gtrsim m_W$, we have the following interactions,[4]

$$\mathcal{L}_{\chi_v,\rm SM} = \frac{c_{\chi 1}}{m_W}\bar{\chi}_v\sigma_\perp^{\mu\nu}\chi_v F_{\mu\nu} + \frac{c_{\chi 2}}{m_W}\bar{\chi}_v\sigma_\perp^{\mu\nu}\chi_v\tilde{F}_{\mu\nu} + \sum_{q=u,d,s,c,b}\left\{ \frac{c_{\chi 3,q}}{m_W^2}\epsilon_{\mu\nu\rho\sigma}v^\mu\bar{\chi}_v\sigma_\perp^{\nu\rho}\chi_v\bar{q}\gamma^\sigma q \right.$$
$$\left. + \frac{c_{\chi 4,q}}{m_W^2}\epsilon_{\mu\nu\rho\sigma}v^\mu\bar{\chi}_v\sigma_\perp^{\nu\rho}\chi_v\bar{q}\gamma^\sigma\gamma_5 q + \frac{c_{\chi 5,q}}{m_W^2}\bar{\chi}_v\chi_v\bar{q}\not{v}\, q + \frac{c_{\chi 6,q}}{m_W^2}\bar{\chi}_v\chi_v\bar{q}\not{v}\,\gamma_5 q + \frac{c_{\chi 7,q}}{m_W^3}\bar{\chi}_v\chi_v m_q\bar{q}q \right.$$

[4] It is convenient to notice the identities, $G^{A\mu\alpha}\tilde{G}^{A\nu}{}_\alpha = g^{\mu\nu}G^{A\alpha\beta}\tilde{G}^A_{\alpha\beta}/4$ and $v_\mu v_\nu G^{A\mu}{}_{[\alpha}\tilde{G}^{A\nu}{}_{\beta]} = -\epsilon_{\alpha\beta}{}^{\mu\nu}v_\mu v^\rho G^A_{\nu\sigma}G^{A\,\sigma}_\rho/2$.

$$
\begin{aligned}
&+\frac{c_{\chi 8,q}}{m_W^3}\bar\chi_v\chi_v\bar q\not v\, iv\cdot D_- q+\frac{c_{\chi 9,q}}{m_W^3}\bar\chi_v\chi_v m_q\bar q i\gamma_5 q+\frac{c_{\chi 10,q}}{m_W^3}\bar\chi_v\chi_v\bar q\not v\,\gamma_5 iv\cdot D_- q\\
&+\frac{c_{\chi 11,q}}{m_W^3}\bar\chi_v\sigma_\perp^{\mu\nu} i\partial_{-\mu}^\perp\chi_v\bar q\gamma_\nu q+\frac{c_{\chi 12,q}}{m_W^3}\epsilon_{\mu\nu\rho\sigma}\bar\chi_v\sigma_\perp^{\mu\nu} i\partial_-^{\perp\rho}\chi_v\bar q\gamma^\sigma q+\frac{c_{\chi 13,q}}{m_W^3}\bar\chi_v\sigma_\perp^{\mu\nu} i\partial_{-\mu}^\perp\chi_v\bar q\gamma_\nu\gamma_5 q\\
&+\frac{c_{\chi 14,q}}{m_W^3}\epsilon_{\mu\nu\rho\sigma}\bar\chi_v\sigma_\perp^{\mu\nu} i\partial_-^{\perp\rho}\chi_v\bar q\gamma^\sigma\gamma_5 q+\frac{c_{\chi 15,q}}{m_W^3}\epsilon_{\mu\nu\rho\sigma}v^\mu\bar\chi_v\sigma_\perp^{\nu\rho}\chi_v\,\bar q(\not v\, iD_-^\sigma+\gamma^\sigma iv\cdot D_-)q\\
&+\frac{c_{\chi 16,q}}{m_W^3}\epsilon_{\mu\nu\rho\sigma}v^\mu\bar\chi_v\sigma_\perp^{\nu\rho}\chi_v\bar q(\not v\, iD_-^\sigma+\gamma^\sigma iv\cdot D_-)\gamma_5 q+\frac{c_{\chi 17,q}}{m_W^3}\bar\chi_v i\partial_-^{\perp\mu}\chi_v\bar q\gamma_\mu q\\
&+\frac{c_{\chi 18,q}}{m_W^3}\bar\chi_v\sigma_\perp^{\mu\nu}\partial_{+\mu}^\perp\chi_v\bar q\gamma_\nu q+\frac{c_{\chi 18,q}}{m_W^3}\epsilon_{\mu\nu\rho\sigma}\bar\chi_v\sigma_\perp^{\mu\nu}\partial_+^{\perp\rho}\chi_v\bar q\gamma^\sigma q+\frac{c_{\chi 20,q}}{m_W^3}\bar\chi_v i\partial_-^{\perp\mu}\chi_v\bar q\gamma_\mu\gamma_5 q\\
&+\frac{c_{\chi 21,q}}{m_W^3}\bar\chi_v\sigma_\perp^{\mu\nu}\partial_{+\mu}^\perp\chi_v\bar q\gamma_\nu\gamma_5 q+\frac{c_{\chi 22,q}}{m_W^3}\epsilon_{\mu\nu\rho\sigma}\bar\chi_v\sigma_\perp^{\mu\nu}\partial_+^{\perp\rho}\chi_v\bar q\gamma^\sigma\gamma_5 q+\frac{c_{\chi 23,q}}{m_W^3}\bar\chi_v\sigma_\perp^{\mu\nu}\chi_v m_q\bar q\sigma_{\mu\nu}q\\
&+\frac{c_{\chi 24,q}}{m_W^3}\epsilon_{\mu\nu\rho\sigma}\bar\chi_v\sigma_\perp^{\mu\nu}\chi_v m_q\bar q\sigma^{\rho\sigma}q\Bigg\}+\frac{c_{\chi 25}}{m_W^3}\bar\chi_v\chi_v G^A_{\alpha\beta}G^{A\alpha\beta}+\frac{c_{\chi 26}}{m_W^3}\bar\chi_v\chi_v G^A_{\alpha\beta}\tilde G^{A\alpha\beta}\\
&+\frac{c_{\chi 27}}{m_W^3}\bar\chi_v\chi_v v_\mu v_\nu G^{A\mu}{}_\alpha G^{A\nu\alpha}+\frac{c_{\chi 28}}{m_W^3}\bar\chi_v\sigma_\perp^{\mu\nu}\chi_v\epsilon_{\mu\nu\alpha\beta}v^\alpha v^\gamma G^{A\beta\delta}G^A_{\gamma\delta}+\dots\,, \qquad (7)
\end{aligned}
$$

where the ellipsis denotes operators of dimension six and higher involving the photon, and operators of dimension eight and higher involving quarks and gluons. In each of (5), (6) and (7) we have employed field redefinitions and chosen a basis of Hermitian QCD operators as in the following Section 3.1.[5] Lorentz-invariance constraints on the coefficients in Eq. (7) may be derived by performing an infinitesimal boost,

$$
\mathcal{B}(q)^\mu{}_\nu = g^\mu{}_\nu+\frac{v^\mu q_\nu-q^\mu v_\nu}{M}+\mathcal{O}(q^2)\,. \qquad (8)
$$

Relativistic fields transform in the usual way, while the heavy field χ_v transforms as [35, 33]

$$
\chi_v(x)\to e^{iq\cdot x}\left[1+\frac{iq\cdot D_\perp}{2M^2}+\frac{1}{4M^2}\sigma_{\alpha\beta}q^\alpha D_\perp^\beta\dots\right]\chi_v(\mathcal{B}^{-1}x)\,, \qquad (9)
$$

where the ellipsis denotes terms higher order in $1/M$. Working through $\mathcal{O}(M^{-1})$ for photon operators and $\mathcal{O}(M^{-3})$ for quark and gluon operators, we find that the variation of Eq. (7) under the boost transformation vanishes upon enforcing the constraints

$$
\frac{m_W}{M}c_{\chi 3}+2c_{\chi 12}=\frac{m_W}{M}c_{\chi 4}+2c_{\chi 14}=\frac{m_W}{M}c_{\chi 5}-2c_{\chi 17}=\frac{m_W}{M}c_{\chi 6}-2c_{\chi 20}=c_{\chi 11}=c_{\chi 13}=0\,, \qquad (10)
$$

where the subscript q on coefficients of quark operators is suppressed. This leaves sixteen independent quark operators (for each quark flavor) through dimension seven, which reduce, upon imposing parity and time-reversal symmetry, to the seven operators describing nucleon-lepton interactions in NRQED [36].

The basis for a heavy scalar is obtained by omitting in Eq. (7) operators containing the spin structure $\sigma_\perp^{\mu\nu}$. The basis for a self-conjugate heavy particle is obtained by imposing invariance under Eq. (3) or Eq. (4); in particular we find that the coefficients $c_{\chi n}$ vanish for n=1, 2, 5, 6, 15, 16, 17, 18, 19, 20, 21, 22, 23, 24.

[5] For the dimension four QCD operators, field redefinitions implement the equations of motion $m_q\bar q\sigma^{\mu\nu}q=\partial^{[\mu}\bar q\gamma^{\nu]}q+\frac{1}{2}\epsilon^{\mu\nu\alpha\beta}\bar q\gamma_\mu iD_{-\nu}\gamma_5 q$ and $\bar q\gamma^{[\mu}iD_-^{\nu]}q=\frac{1}{2}\epsilon^{\mu\nu\alpha\beta}\partial_\alpha(\bar q\gamma_\sigma\gamma_5 q)$.

2.4 Weak scale matching

Above the weak scale, the theory for the WIMP, symmetric under $SU(3)_c \times SU(2)_W \times U(1)_Y$, may be specified in terms of a renormalizable UV completion (e.g., a supersymmetric extension), a basis of contact operators in the case of a heavy mediator, or heavy particle effective theory in the case of a heavy WIMP. By performing a matching calculation between the theories above and below the weak scale, thereby integrating out the weak scale particles including $W^\pm, Z^0, t, h$, we obtain a solution for the coefficients c_i of the low-energy effective theories in Eqs. (5), (6), or (7) in terms of parameters in the high-energy theory.

As a simple illustration, let us consider the case of a Majorana fermion electroweak singlet. The lowest dimension operators involving SM interactions are given in the electroweak symmetric theory by

$$\mathcal{L}_{\psi,\mathrm{SM}} = \frac{1}{2}\bar{\psi}\left(i\partial\!\!\!/ - M'\right)\psi - \frac{1}{\Lambda}\bar{\psi}\left(c'_{\psi 1} + ic'_{\psi 2}\gamma_5\right)\psi H^\dagger H + \dots\,, \tag{11}$$

where the ellipsis denotes terms suppressed by higher powers of Λ, the scale associated with a heavy mediator. Let us further assume ψ to have mass parameter $M' \ll m_W$, and hence organize the matching by a power counting employing a scale separation $M' \ll m_W \ll \Lambda$.

Upon integrating out the physical Higgs field h and the top quark t, and performing the field redefinition,

$$\psi \to e^{-i\phi\gamma_5}\psi\,, \quad \tan 2\phi = \frac{c'_{\psi 2}v^2}{c'_{\psi 1}v^2 + M'\Lambda}\,, \tag{12}$$

to retain a positive real mass convention for ψ, we obtain the effective lagrangian below the weak scale

$$\mathcal{L}_{\psi,\mathrm{SM}} = \frac{1}{2}\bar{\psi}\left(i\partial\!\!\!/ - M\right)\psi + \frac{1}{m_W^3}\left[\bar{\psi}\left(c_{\psi 7} + ic_{\psi 8}\gamma_5\right)\psi\sum_q m_q\bar{q}q + \bar{\psi}\left(c_{\psi 17} + ic_{\psi 18}\gamma_5\right)\psi\, G^A_{\mu\nu}G^{A\mu\nu}\right] + \dots\,, \tag{13}$$

where the sum runs over the active quark mass eigenstates $q = u, d, s, c, b$, and the ellipsis denotes higher-order perturbative and power corrections. The physical DM mass and the effective couplings in the low energy theory are given at leading order by

$$\begin{aligned} M &= \sqrt{\left(M' + \frac{c'_{\psi 1}v^2}{\Lambda}\right)^2 + \left(\frac{c'_{\psi 2}v^2}{\Lambda}\right)^2}\,, \\ \{c_{\psi 7}\,, c_{\psi 8}\} &= \frac{m_W^3 M'}{m_h^2\Lambda M}\left\{c'_{\psi 1} + \frac{v^2}{M'\Lambda}\left[c'^2_{\psi 1} + c'^2_{\psi 2}\right], c'_{\psi 2}\right\}\,, \quad \{c_{\psi 17}\,, c_{\psi 18}\} = -\frac{\alpha_s(m_W)}{12\pi}\{c_{\psi 7}\,, c_{\psi 8}\}\,. \end{aligned} \tag{14}$$

Note that a vanishing $c'_{\psi 1}$ does not imply a velocity-suppressed spin-independent cross section for WIMP nucleon scattering, since a nonvanishing $c_{\psi 8} \sim (v^2/M'\Lambda)c'^2_{\psi 2}$ is induced in the low energy theory.[6] While we do not pursue a detailed phenomenology of the model (13), this example illustrates some generic features of weak scale matching. Firstly, particular UV completions may have nontrivial correlations and suppression factors amongst coefficients; e.g., $c_{3,4,9,10}$ are suppressed by loop ($\sim g^2$)

[6] This observation has been employed in [37, 18]. Also, spin-dependent interactions may generate spin-independent interactions at loop level [38].

d	QCD operator basis
3	$V_q^\mu = \bar{q}\gamma^\mu q$
	$A_q^\mu = \bar{q}\gamma^\mu\gamma_5 q$
4	$T_q^{\mu\nu} = im_q\bar{q}\sigma^{\mu\nu}\gamma_5 q$
	$O_q^{(0)} = m_q\bar{q}q\,, \quad O_g^{(0)} = G^A_{\mu\nu}G^{A\mu\nu}$
	$O_{5q}^{(0)} = m_q\bar{q}i\gamma_5 q\,, \quad O_{5g}^{(0)} = \epsilon^{\mu\nu\rho\sigma}G^A_{\mu\nu}G^A_{\rho\sigma}$
	$O_q^{(2)\mu\nu} = \frac{1}{2}\bar{q}\left(\gamma^{\{\mu}iD_-^{\nu\}} - \frac{g^{\mu\nu}}{4}i\not{D}_-\right)q\,, \quad O_g^{(2)\mu\nu} = -G^{A\mu\lambda}G^{A\nu}{}_\lambda + \frac{g^{\mu\nu}}{4}(G^A_{\alpha\beta})^2$
	$O_{5q}^{(2)\mu\nu} = \frac{1}{2}\bar{q}\gamma^{\{\mu}iD_-^{\nu\}}\gamma_5 q$

Table 2: The seven operator classes: vector $\left(V_q\right)$, axial-vector $\left(A_q\right)$, tensor $\left(T_q\right)$, scalar $\left(O_q^{(0)}, O_g^{(0)}\right)$, pseudoscalar $\left(O_{5q}^{(0)}, O_{5g}^{(0)}\right)$, C-even spin-2 $\left(O_q^{(2)}, O_g^{(2)}\right)$ and C-odd spin-2 $\left(O_{5q}^{(2)}\right)$. Here $A^{[\mu}B^{\nu]} \equiv (A^\mu B^\nu - A^\nu B^\mu)/2$ and $A^{\{\mu}B^{\nu\}} \equiv (A^\mu B^\nu + A^\nu B^\mu)/2$ respectively denote antisymmetrization and symmetrization, and the subscript q denotes an active quark flavor. The antisymmetric tensor current T_q and the quark pseudoscalar operator $O_{5q}^{(0)}$ both include a conventional quark mass prefactor.

or power ($\sim 1/\Lambda$) corrections. Secondly, effects that are naively absent from the high scale lagrangian are nonetheless present once a complete analysis is performed. It is essential to include a complete basis that is closed under renormalization and contains all operators not forbidden by symmetry.

Weak scale matching for an electroweak singlet Dirac fermion or (real or complex) scalar can be similarly performed. Weak scale matching for the case of electroweak charged dark matter, requires a more intricate analysis as detailed in Ref. [4].

3 Operator renormalization, scale evolution and matching at heavy quark thresholds

Having determined the basis of effective operators and their coefficients at the weak scale, we may proceed to map onto a theory valid at lower energy scales. We identify the relevant QCD operators and compute their anomalous dimensions. We then solve the corresponding renormalization group evolution equations and enforce matching conditions at heavy quark thresholds, passing from $n_f = 5$ renormalized at $\mu \sim m_W$ to $n_f = 3$ (or $n_f = 4$) renormalized below the charm (or bottom) threshold.

3.1 QCD operator basis

Inspection of the low-energy SM building blocks in (1) shows that, up to field redefinitions, the strong interaction matrix elements relevant for WIMP-SM interactions through dimension seven involve seven QCD operator classes collected in Table 2: at dimension three we have the vector and axial-vector currents; at dimension four we have the antisymmetric tensor currents, the scalar operators, the pseudoscalar operators, the C-even spin-2 operators and the C-odd spin-2 operators. Each of these classes transforms irreducibly under continuous and discrete Lorentz transformations, and is separately closed under renormalization.

Operator	Renormalization constant
V_q	$Z_V = 1$
A_q	$Z_A^{(\text{singlet})} = 1 + \frac{\alpha_s}{4\pi}\frac{16}{3} - \left(\frac{\alpha_s}{4\pi}\right)^2 \frac{1}{\epsilon}\left(\frac{20}{9}n_f + \frac{88}{3}\right) + \mathcal{O}(\alpha_s^3)\,,$ $Z_A^{(\text{non-singlet})} = 1 + \frac{\alpha_s}{4\pi}\frac{16}{3} + \left(\frac{\alpha_s}{4\pi}\right)^2 \frac{1}{\epsilon}\left(\frac{16}{9}n_f - \frac{88}{3}\right) + \mathcal{O}(\alpha_s^3)$
T_q	$Z_T = 1 - \frac{\alpha_s}{4\pi}\frac{1}{\epsilon}\frac{16}{3} + \mathcal{O}(\alpha_s^2)$
$O_q^{(0)}\,, O_g^{(0)}$	$Z_{qq}^{(0)} = 1\,, \quad Z_{qg}^{(0)} = 0\,,$ $Z_{gq}^{(0)} = \frac{2\gamma_m}{\epsilon}\,, \quad Z_{gg}^{(0)} = 1 - \frac{\tilde{\beta}}{\epsilon}$
$O_{5q}^{(0)}\,, O_{5g}^{(0)}$	$Z_{5,qq}^{(0)} = 1 + \frac{\alpha_s}{4\pi}\frac{32}{3} + \mathcal{O}(\alpha_s^2)\,, \quad Z_{5,qg}^{(0)} = 0 + \mathcal{O}(\alpha_s^2)\,,$ $Z_{5,gq}^{(0)} = \frac{\alpha_s}{4\pi}\frac{1}{\epsilon}16 + \mathcal{O}(\alpha_s^2)\,, \quad Z_{5,gg}^{(0)} = 1 + \frac{\alpha_s}{4\pi}\frac{1}{\epsilon}\beta_0 + \mathcal{O}(\alpha_s^2)$
$O_q^{(2)}\,, O_g^{(2)}$	$Z_{qq}^{(2)} = 1 - \frac{\alpha_s}{4\pi}\frac{1}{\epsilon}\frac{32}{9} + \mathcal{O}(\alpha_s^2)\,, \quad Z_{qg}^{(2)} = \frac{\alpha_s}{4\pi}\frac{1}{\epsilon}\frac{2}{3} + \mathcal{O}(\alpha_s^2)\,,$ $Z_{gq}^{(2)} = \frac{\alpha_s}{4\pi}\frac{1}{\epsilon}\frac{32}{9} + \mathcal{O}(\alpha_s^2)\,, \quad Z_{gg}^{(2)} = 1 - \frac{\alpha_s}{4\pi}\frac{1}{\epsilon}\frac{2n_f}{3} + \mathcal{O}(\alpha_s^2)$
$O_{5q}^{(2)}$	$Z_5^{(2)} = 1 - \frac{\alpha_s}{4\pi}\frac{1}{\epsilon}\frac{32}{9} + \mathcal{O}(\alpha_s^2)$

Table 3: Renormalization constants for each of the seven operator classes arising in the low-energy effective theory for the DM particle. Here n_f is the number of active quark flavors and $\beta_0 = 11 - 2n_f/3$.

3.2 Renormalization constants

Let us denote by O_i a generic operator with coefficient c_i belonging to one of the seven operator classes closed under renormalization. The relations between bare and renormalized operators and coefficients are given by

$$O_i^{\text{bare}} = Z_{ij}(\mu) O_j^{\text{ren}}(\mu)\,, \quad c_i^{\text{ren}}(\mu) = Z_{ji}(\mu) c_j^{\text{bare}}\,, \tag{15}$$

with an implicit sum over repeated indices. We define the operator renormalization constants Z_{ij} in the $\overline{\text{MS}}$ scheme, except for the axial-vector and pseudoscalar operators where we consider an additional finite renormalization to retain a conventional axial current divergence and the scale independence of the quark pseudoscalar matrix elements.

For vector currents, axial-vector currents, tensor currents and C-odd spin-two operators, the renormalization constants are quark flavor diagonal, and have the form $Z_{ij} = Z\delta_{ij}$, with Z listed in Table 3. For scalar, pseudoscalar and C-even spin-two operators, the renormalization constants, in the basis $(u, d, s, \ldots | g)$, have the form

$$Z = \left(\begin{array}{ccc|c} Z_{qq} & & & Z_{qg} \\ & \ddots & & \vdots \\ & & Z_{qq} & Z_{qg} \\ \hline Z_{gq} & \cdots & Z_{gq} & Z_{gg} \end{array}\right)\,, \tag{16}$$

with elements Z_{ij} listed in Table 3.

The vector currents, representing conserved quark number, $\partial_\mu V_q^\mu = 0$, evolve trivially under QCD renormalization. For the axial-vector currents, we consider separately the quark-flavor singlet and non-singlet combinations (see Eq. (48)), and work in the 't Hooft-Veltman scheme with the convention $\epsilon^{0123} = +1$,

$$\gamma_5 = i\gamma^0\gamma^1\gamma^2\gamma^3 = -\frac{i}{4!}\epsilon^{\mu\nu\rho\sigma}\gamma_\mu\gamma_\nu\gamma_\rho\gamma_\sigma \,. \tag{17}$$

The renormalization constants $Z_A^{(\mathrm{singlet})}$ and $Z_A^{(\mathrm{non-singlet})}$ include a finite correction in addition to the $\overline{\mathrm{MS}}$ scheme [39] (see Appendix A for details), which retains the one-loop anomaly condition,

$$\sum_q \partial_\mu A_q^\mu = \sum_q 2im_q\bar{q}\gamma_5 q - \frac{g^2 n_f}{32\pi^2}\epsilon^{\mu\nu\rho\sigma}G^a_{\mu\nu}G^a_{\rho\sigma} \,, \tag{18}$$

for the singlet combination, and imposes a vanishing anomalous dimension for the non-singlet combination. Terms contributing to the one-loop matching and two-loop anomalous dimension have been retained in both $Z_A^{(\mathrm{non-singlet})}$ and $Z_A^{(\mathrm{singlet})}$. Corrections through three-loop order are also available [39].

For the tensor current, the renormalization constant includes the contribution Z_m (given in Appendix A) from the quark mass appearing in the definition of T_q. Two loop corrections to Z_T are also available [40, 41, 42]. For the scalar operators, the all-orders expression for the coefficient of the $1/\epsilon$ term of $Z^{(0)}$ is specified in terms of coupling and mass renormalization functions,[7]

$$\tilde{\beta} = \beta/g \,, \quad \beta = \frac{dg}{d\log\mu} \,, \quad \gamma_m = \frac{d\log m_q}{d\log\mu} \,, \tag{19}$$

which are given explicitly in Appendix A.

For the pseudoscalar operators, we employ the γ_5 scheme in Eq. (17), and have included the contribution Z_m from the quark mass appearing in the definition of $O_{5q}^{(0)}$. The renormalization constant $Z_5^{(0)}$ also includes an additional finite renormalization constant that ensures nonrenormalization of the pseudoscalar quark operators [39] (see Appendix A for details). Terms contributing to the one-loop matching and two-loop anomalous dimension have been retained in $Z_5^{(0)}$. For the C-even spin-two operators, three-loop corrections to the renormalization constant are available from Refs. [43, 44]. For the C-odd spin-two operators, the two-loop anomalous dimension may be obtained from Ref. [45].

3.3 Anomalous dimensions and renormalization group evolution

From the relations between bare and renormalized quantities in Eq. (15), we obtain the scale evolution equations

$$\frac{d}{d\log\mu}O_i = -\gamma_{ij}O_j \,, \quad \frac{d}{d\log\mu}c_i = \gamma_{ji}c_j \,, \quad \gamma_{ij} \equiv Z^{-1}_{ik}\frac{d}{d\log\mu}Z_{kj} \,, \tag{20}$$

where the scale dependence and superscript "ren" on renormalized quantities in (15) have been suppressed, and we have defined the anomalous dimension matrix γ_{ij}. In the $\overline{\mathrm{MS}}$ scheme the anomalous dimension is given to all orders in α_s in terms of the coefficient of $1/\epsilon$ in Z_{ij},

$$\gamma_{ij} = -g\frac{\partial}{\partial g}Z_{(1)ij} \,, \quad Z_{ij} = \delta_{ij} + \sum_{n=1}^{\infty}\frac{Z_{(n)ij}}{\epsilon^n} \,. \tag{21}$$

[7] A typo appears in the expression after equation (24) of [15], which should read $g^{-1}\beta = g^{-1}dg/d\log\mu \approx -\beta_0\alpha_s/4\pi$.

Operator	Anomalous dimension
V_q	$\gamma_V = 0$
A_q	$\gamma_A^{(\text{singlet})} = \left(\frac{\alpha_s}{4\pi}\right)^2 16 n_f + \mathcal{O}(\alpha_s^3)\,,$ $\gamma_A^{(\text{non-singlet})} = 0$
T_q	$\gamma_T = -\frac{\alpha_s}{4\pi}\frac{32}{3} + \mathcal{O}(\alpha_s^2)\,,$
$O_q^{(0)}\,, O_g^{(0)}$	$\gamma_{qq}^{(0)} = 0\,, \quad \gamma_{qg}^{(0)} = 0\,,$ $\gamma_{gq}^{(0)} = -2\gamma_m'\,, \quad \gamma_{gg}^{(0)} = \tilde{\beta}'$
$O_{5q}^{(0)}\,, O_{5g}^{(0)}$	$\gamma_{5,qq}^{(0)} = 0\,, \quad \gamma_{5,qg}^{(0)} = 0\,,$ $\gamma_{5,gq}^{(0)} = -\frac{\alpha_s}{4\pi} 32 + \mathcal{O}(\alpha_s^2)\,, \quad \gamma_{5,gg}^{(0)} = -\frac{\alpha_s}{4\pi} 2\beta_0 + \mathcal{O}(\alpha_s^2)$
$O_q^{(2)}\,, O_g^{(2)}$	$\gamma_{qq}^{(2)} = \frac{\alpha_s}{4\pi}\frac{64}{9} + \mathcal{O}(\alpha_s^2)\,, \quad \gamma_{qg}^{(2)} = -\frac{\alpha_s}{4\pi}\frac{4}{3} + \mathcal{O}(\alpha_s^2)\,,$ $\gamma_{gq}^{(2)} = -\frac{\alpha_s}{4\pi}\frac{64}{9} + \mathcal{O}(\alpha_s^2)\,, \quad \gamma_{gg}^{(2)} = \frac{\alpha_s}{4\pi}\frac{4n_f}{3} + \mathcal{O}(\alpha_s^2)$
$O_{5q}^{(2)}$	$\gamma_5^{(2)} = \frac{\alpha_s}{4\pi}\frac{64}{9} + \mathcal{O}(\alpha_s^2)$

Table 4: Anomalous dimensions for the seven operator classes arising in the low-energy effective theory for the DM particle. Here we denote $X' \equiv g\frac{\partial}{\partial g}X$.

The renormalization constants for axial-vector currents and pseudoscalar operators include a finite contribution beyond $\overline{\text{MS}}$, and hence we employ the general definition in (20) to determine their anomalous dimensions.

For vector currents, axial-vector currents, tensor currents and C-odd spin-two operators, the anomalous dimensions have the form $\gamma_{ij} = \gamma\delta_{ij}$, with γ listed in Table 4. For scalar, pseudoscalar and C-even spin-two operators, the anomalous dimensions, in the basis $(u, d, s, \ldots | g)$, have the form

$$\gamma = \left(\begin{array}{ccc|c} \gamma_{qq} & & & \gamma_{qg} \\ & \ddots & & \vdots \\ & & \gamma_{qq} & \gamma_{qg} \\ \hline \gamma_{gq} & \cdots & \gamma_{gq} & \gamma_{gg} \end{array}\right)\,. \tag{22}$$

with elements γ_{ij} listed in Table 4.

It is straightforward to solve for the evolution of coefficients from a high scale μ_h down to a low scale μ_l, employing the anomalous dimension for each of the seven operator classes. Let us express the solutions as

$$c_i(\mu_l) = R_{ij}(\mu_l, \mu_h) c_j(\mu_h)\,. \tag{23}$$

For vector currents, axial-vector currents, tensor currents and C-odd spin-two operators, the solutions have the form $R_{ij} = R\delta_{ij}$, with R listed in Table 5. For scalar, pseudoscalar operators and C-even

Operator	Solution to coefficient running
V_q	$R_V = 1$
A_q	$R_A^{(\text{singlet})} = \exp\left\{\frac{2n_f}{\pi\beta_0}\left[\alpha_s(\mu_h) - \alpha_s(\mu_l)\right] + \mathcal{O}(\alpha_s^2)\right\}$, $R_A^{(\text{non-singlet})} = 1$
T_q	$R_T = \left(\frac{\alpha_s(\mu_l)}{\alpha_s(\mu_h)}\right)^{-\frac{16}{3\beta_0}}\left[1 + \mathcal{O}(\alpha_s)\right]$
$O_q^{(0)}, O_g^{(0)}$	$R_{qq}^{(0)} = 1\,, \quad R_{qg}^{(0)} = 2[\gamma_m(\mu_h) - \gamma_m(\mu_l)]/\tilde{\beta}(\mu_h)\,,$ $R_{gq}^{(0)} = 0\,, \quad R_{gg}^{(0)} = \tilde{\beta}(\mu_l)/\tilde{\beta}(\mu_h)$
$O_{5q}^{(0)}, O_{5g}^{(0)}$	$R_{5,qq}^{(0)} = 1\,, \quad R_{5,qg}^{(0)} = \frac{16}{\beta_0}\left(\frac{\alpha_s(\mu_l)}{\alpha_s(\mu_h)} - 1\right) + \mathcal{O}(\alpha_s)\,,$ $R_{5,gq}^{(0)} = 0\,, \quad R_{5,gg}^{(0)} = \frac{\alpha_s(\mu_l)}{\alpha_s(\mu_h)} + \mathcal{O}(\alpha_s)$
$O_q^{(2)}, O_g^{(2)}$	$R_{qq}^{(2)} - R_{qq'}^{(2)} = r(0) + \mathcal{O}(\alpha_s)\,, \quad R_{qq'}^{(2)} = \frac{1}{n_f}\left[\frac{16r(n_f)+3n_f}{16+3n_f} - r(0)\right] + \mathcal{O}(\alpha_s)\,,$ $R_{qg}^{(2)} = \frac{16[1-r(n_f)]}{16+3n_f} + \mathcal{O}(\alpha_s)\,,$ $R_{gq}^{(2)} = \frac{3[1-r(n_f)]}{16+3n_f} + \mathcal{O}(\alpha_s)\,, \quad R_{gg}^{(2)} = \frac{16+3n_f r(n_f)}{16+3n_f} + \mathcal{O}(\alpha_s)$
$O_{5q}^{(2)}$	$R_5^{(2)} = \left(\frac{\alpha_s(\mu_l)}{\alpha_s(\mu_h)}\right)^{-\frac{32}{9\beta_0}}\left[1 + \mathcal{O}(\alpha_s)\right]$

Table 5: Solutions to coefficient running for each of the seven operator classes arising in the low-energy effective theory for the DM particle. The coefficient running for C-even spin-two operators are given in terms of the function $r(t)$ defined in Eq. (25).

spin-two operators, the solutions in the basis $(u, d, s, \ldots | g)$ have the form

$$R = \left(\begin{array}{ccc|c} & & & R_{qg} \\ & \mathbb{1}(R_{qq} - R_{qq'}) + \mathbb{J}R_{qq'} & & \vdots \\ & & & R_{qg} \\ \hline R_{gq} & \cdots & R_{gq} & R_{gg} \end{array}\right), \tag{24}$$

where the $n_f \times n_f$ matrices $\mathbb{1}$ and $\mathbb{J}$ are respectively the identity matrix and the matrix with all elements equal to unity. For the scalar and pseudoscalar operators $R_{qq'} = 0$. The elements R_{ij} are specified in Table 5, where the results for the C-even spin-two operators involve the function

$$r(t) = \left(\frac{\alpha_s(\mu_l)}{\alpha_s(\mu_h)}\right)^{-\frac{1}{2\beta_0}\left(\frac{64}{9} + \frac{4}{3}t\right)}. \tag{25}$$

The vector and non-singlet axial-vector currents have vanishing anomalous dimension, and hence trivial scale evolution. For the singlet axial-vector current, non-trivial renormalization begins at

Operator	Solution to matching condition
V_q	$M_V = 1$
A_q	$M_A = 1 + \mathcal{O}(\alpha_s^2)$
T_q	$M_T = 1 + \mathcal{O}(\alpha_s^2)$
$O_q^{(0)}, O_g^{(0)}$	$M_{gQ}^{(0)} = -\frac{\alpha_s'(\mu_Q)}{12\pi}\left\{1 + \frac{\alpha_s'(\mu_Q)}{4\pi}\left[11 - \frac{4}{3}\log\frac{\mu_Q}{m_Q}\right] + \mathcal{O}(\alpha_s^2)\right\}$, $M_{gg}^{(0)} = 1 - \frac{\alpha_s'(\mu_Q)}{3\pi}\log\frac{\mu_Q}{m_Q} + \mathcal{O}(\alpha_s^2)$
$O_{5q}^{(0)}, O_{5g}^{(0)}$	$M_{5,gQ}^{(0)} = \frac{\alpha_s'(\mu_Q)}{8\pi} + \mathcal{O}(\alpha_s^2)$, $\quad M_{5,gg}^{(0)} = 1 + \mathcal{O}(\alpha_s)$
$O_q^{(2)}, O_g^{(2)}$	$M_{gQ}^{(2)} = \frac{\alpha_s'}{3\pi}\log\frac{\mu_Q}{m_Q} + \mathcal{O}(\alpha_s^2)$, $\quad M_{gg}^{(2)} = 1 + \mathcal{O}(\alpha_s)$
$O_{5q}^{(2)}$	$M_5^{(2)} = 1 + \mathcal{O}(\alpha_s^2)$

Table 6: Heavy quark threshold matching relations for the seven operator classes. The strong coupling in the (n_f+1)-flavor theory is denoted α_s'.

two-loop. For the tensor current and C-odd spin-two operator we have presented the leading logarithmic order solutions. The chosen renormalization prescription ensures scale invariance of the quark pseudoscalar operators to all orders.

For most phenomenological applications we may simply evaluate the matrix elements of the C-even spin-two operators in terms of parton distribution functions (PDFs) at the weak scale $\mu_h \sim m_W$. This avoids the need for renormalization group analysis (apart from matching to a convenient scale to evaluate matrix elements) and heavy-quark threshold matching conditions. Nonetheless, we include the above results for future analyses which may require an evaluation of tensor matrix elements at low scales, such as in considering multi-nucleon contributions to matrix elements [46, 26, 47], or in investigating the power-suppressed mixing between scalar and tensor operators.

3.4 Heavy quark threshold matching

After evolving to the scale $\mu_Q \sim m_Q$, we integrate out the heavy quark, i.e., the bottom or charm quark, of mass m_Q. The coefficients in the n_f- and (n_f+1)-flavor theories are related by matching physical matrix elements. In terms of renormalized coefficients and operators the matching condition is

$$c_i'\langle O_i'\rangle = c_i\langle O_i\rangle + \mathcal{O}(1/m_Q)\,, \tag{26}$$

where primed and unprimed quantities are in the (n_f+1)- and n_f-flavor theories, respectively.[8] Let us express the solution to the matching condition as

$$c_i(\mu_Q) = M_{ij}(\mu_Q)c_j'(\mu_Q)\,. \tag{27}$$

[8] For example, the matching condition for scalar operators, between physical matrix elements in the 5- and 4-flavor theories, is given by $c_g^{(0)\prime}\langle O_g^{(0)\prime}\rangle + \sum_{q=u,d,s,c,b} c_q^{(0)\prime}\langle O_q^{(0)\prime}\rangle = c_g^{(0)}\langle O_g^{(0)}\rangle + \sum_{q=u,d,s,c} c_q^{(0)}\langle O_q^{(0)}\rangle + \mathcal{O}(1/m_b)$, where primed and unprimed quantities are in the 5- and 4-flavor theories, respectively, and the scale dependence is implicit.

The vector currents have trivial matching conditions up to power corrections, while the axial-vector currents, tensor currents and C-odd spin-two operators receive threshold matching corrections beginning at $\mathcal{O}(\alpha_s^2)$. Since the latter operator classes have nuclear spin-dependent and/or velocity-suppressed matrix elements in physical WIMP-nucleon processes at small relative velocity, we restrict attention to the leading effects of renormalization scale evolution as detailed in the previous section, and neglect heavy quark threshold matching conditions which are suppressed in each case by a further power of α_s.[9] In terms of Eq. (27), we express these solutions in the basis $(u, d, s, \ldots | Q)$ as the $n_f \times (n_f + 1)$ matrix $M_{ij} = M\delta_{ij}$, with $i = u, d, s, \ldots$ and $j = u, d, s, \ldots, Q$. The constants M are collected in Table 6.

For the scalar, pseudoscalar and C-even spin-two operators, threshold matching involving gluon operators begins at $\mathcal{O}(\alpha_s)$, and the solution to the matching condition may be expressed in terms of an $(n_f + 1) \times (n_f + 2)$ matrix in the basis $(u, d, s, \ldots | Q | g)$ as

$$M = \left(\begin{array}{ccc|c|c} 1 & & & 0 & 0 \\ & \ddots & & \vdots & \vdots \\ & & 1 & 0 & 0 \\ \hline 0 & \cdots & 0 & M_{gQ} & M_{gg} \end{array}\right) . \tag{28}$$

This parameterization is sufficient for matching at NLO for scalar operators [50] and at LO for pseudoscalar and C-even spin-two operators.[10] The elements M_{ij} are given in Table 6. Scheme dependence for the heavy quark mass (e.g. pole versus $\overline{\rm MS}$) appears at higher order.

Due to the lightness of the charm quark, and correspondingly poorly convergent $\alpha_s(m_c)$ expansion, WIMP-nucleon cross sections can depend sensitively on threshold corrections for the scalar operator. Contributions from matrix elements of the heavy quark operator, i.e., the column vector $M^{(0)}_{i(n_f+1)}$, are known through $\mathcal{O}(\alpha_s^3)$ [51]. In the next section, we employ a sum rule for matrix elements of scalar operators, derived from the QCD energy momentum tensor, to obtain new relations amongst the elements of $M^{(0)}$, thus extending the available results at higher-orders.

3.5 Sum rule constraints on scale evolution and heavy quark threshold matching

The equivalence of physical matrix elements determined in theories defined at different scales or with different numbers of active quark flavors, together with the solutions for coefficient evolution and matching at heavy quark thresholds given in Eqs. (23) and (27), imply relations between operator matrix elements:

$$\langle O_i^{\prime(S)} \rangle(\mu_h) = R^{(S)}_{ji}(\mu, \mu_h) \langle O_j^{(S)} \rangle(\mu) \,, \quad \langle O_i^{\prime(S)} \rangle(\mu_b) = M^{(S)}_{ji}(\mu_b) \langle O_j^{(S)} \rangle(\mu_b) + \mathcal{O}(1/m_b) \,, \tag{29}$$

where $\langle \cdot \rangle \equiv \langle N | \cdot | N \rangle$ denotes a physical matrix element (for definiteness we consider the matrix element in a nucleon state $|N\rangle$). The first relation links operator matrix elements at different scales but with the same number of active quarks, while the second relation links operator matrix elements at the same scale (here taken to be the bottom threshold for definiteness) but with $n_f + 1$ (primed) and n_f (unprimed) active flavors.

The matrix elements $\langle O_i^{(S)} \rangle$ are not independent but linked by sum rules derived from the trace and traceless part of the (symmetric and conserved) QCD energy momentum tensor $\theta^{\mu\nu}$. Let us

[9] For explicit results at two and three loop order see [48, 49].

[10] In the next section we generalize the parameterization of M_{ij} for higher-order matching in the case of scalar operators.

focus on the scalar case, $S = 0$, where the sum rule for n_f flavors is given by the trace part as

$$\langle \theta^\mu_\mu \rangle = m_N = (1 - \gamma_m) \sum_{q=u,d,s,\ldots}^{n_f} \langle O_q^{(0)} \rangle + \frac{\tilde{\beta}}{2} \langle O_g^{(0)} \rangle \,. \tag{30}$$

The sum rule relating matrix elements $\langle O_i^{\prime(S)} \rangle$ in a theory with $n_f + 1$ flavors has the analogous form.

Consistency between Eqs. (29) and (30) yields a system of equations which imposes constraints on the matrices $R^{(0)}$ and $M^{(0)}$. In the following, we drop the superscript (0) for brevity. In the case of scale evolution, the sum rule determines R. Starting from the general form,

$$R(\mu, \mu_h) = \left(\begin{array}{ccc|c} 1 & & & R_{qg} \\ & \ddots & & \vdots \\ & & 1 & R_{qg} \\ \hline 0 & \cdots & 0 & R_{gg} \end{array}\right) , \tag{31}$$

which follows from the scale invariance of $\langle O_q^{(0)} \rangle$, the functions R_{qg} and R_{gg} are determined by the system of equations derived from Eqs. (29) and (30):

$$\frac{2}{\tilde{\beta}(\mu)} R_{gg} = \frac{2}{\tilde{\beta}(\mu_h)} \,, \quad R_{qg} - \frac{2}{\tilde{\beta}(\mu)} \big[1 - \gamma_m(\mu)\big] R_{gg} = -\frac{2}{\tilde{\beta}(\mu_h)} \big[1 - \gamma_m(\mu_h)\big] \,. \tag{32}$$

This yields the results given in Table 5.

In the case of heavy quark threshold matching, relations between elements of the matrix M can be similarly derived. Consider the general form,

$$M(\mu_Q) = \left(\begin{array}{ccc|cc} & & & M_{qQ} & M_{qg} \\ & \mathbb{1}(M_{qq} - M_{qq'}) + \mathbb{J} M_{qq'} & & \vdots & \vdots \\ & & & M_{qQ} & M_{qg} \\ \hline M_{gq} & \cdots & M_{gq} & M_{gQ} & M_{gg} \end{array}\right) , \tag{33}$$

where the $n_f \times n_f$ matrices $\mathbb{1}$ and $\mathbb{J}$ are respectively the identity matrix and the matrix with all elements equal to unity. The system of equations derived from Eqs. (29) and (30) yield the following relations

$$\begin{aligned} 0 &= \tilde{\beta}^{(n_f)} - \tilde{\beta}^{(n_f+1)} M_{gg} - 2\big[1 - \gamma_m^{(n_f+1)}\big](M_{gQ} + n_f M_{gq}) \,, \\ 0 &= 2\Big\{1 - \gamma_m^{(n_f)} - \big[1 - \gamma_m^{(n_f+1)}\big](M_{qQ} + M_{qq} + (n_f - 1) M_{qq'})\Big\} - \tilde{\beta}^{(n_f+1)} M_{qg} \,, \end{aligned} \tag{34}$$

where the superscripts on γ_m and $\tilde{\beta}$ denote the n_f dependence, while the μ_Q dependence is implicit.

We may further simplify the matrix (33). By dimensional analysis, the gauge invariant operator $m_q \bar{q} q$ matches onto $(G^A_{\mu\nu})^2$ with power suppression, $\sim m_q/m_Q$, and hence $M_{gq} \equiv 0$. Conserved global chiral symmetries, $q_{L,R} \to e^{i\epsilon_{L,R}} q_{L,R}$ when $m_q \to 0$, imply that integrating out the heavy quark Q in the presence of $m_q \bar{q} q$ does not induce $m_{q'} \bar{q}' q'$ for $q' \neq q$, i.e., $M_{qq'} \equiv 0$.[11] Finally, since the quark

[11] We are free to assume here an anticommuting γ_5 prescription, since γ_5 does not enter the QCD analysis of the scalar operators. The assumption of diagonal quark matching underlies the light quark mass decoupling analysis [51, 52]. For an explicit comparison of decoupling relations for pseudoscalar and axial currents using different γ_5 prescriptions, see [49].

masses in the n_f and $n_f - 1$ flavor theories are defined to include the induced effects of the heavy quark, we have simply $M_{qq} \equiv 1$. These arguments imply from (33) a solution for all elements in terms of M_{gQ} and M_{qQ}:

$$\begin{aligned}
&M_{qq} \equiv 1\,, \quad M_{qq'} \equiv 0\,, \quad M_{gq} \equiv 0\,,\\
&M_{gg} = \frac{\tilde\beta^{(n_f)}}{\tilde\beta^{(n_f+1)}} - \frac{2}{\tilde\beta^{(n_f+1)}}\big[1-\gamma_m^{(n_f+1)}\big] M_{gQ}\,,\\
&M_{gq} = \frac{2}{\tilde\beta^{(n_f+1)}}\big[\gamma_m^{(n_f+1)} - \gamma_m^{(n_f)}\big] - \frac{2}{\tilde\beta^{(n_f+1)}}\big[1-\gamma_m^{(n_f+1)}\big] M_{qQ}\,.
\end{aligned} \tag{35}$$

Let us consider solutions for the elements of $M^{(0)}$ expanded in powers of α_s,

$$M = \sum_{n=0}^{\infty} \left(\frac{\alpha_s^{(n_f+1)}(\mu_Q)}{\pi}\right)^n M^{(n)}\,, \tag{36}$$

where the superscript signifies that the strong coupling constant is defined in the (n_f+1)-flavor theory. Employing this α_s counting and the $\mathcal{O}(\alpha_s^4)$ results for M_{gQ} and M_{qQ} from Ref. [51], we may solve the relations in Eq. (34) order by order.[12] Let us work in the $\overline{\rm MS}$ scheme, employing results for M_{gQ} and M_{qQ}, as well as for the nontrivial matching condition between $\alpha_s^{(n_f)}(\mu_Q)$ and $\alpha_s^{(n_f+1)}(\mu_Q)$ found in Ref. [51], expressed in terms of the heavy quark mass m_Q defined in this scheme. Working through NLO, we recover the result in Table 6. At NNLO, we find

$$M_{gg}^{(2)} = \frac{11}{36} - \frac{11}{6}\log\frac{\mu_Q}{m_Q} + \frac{1}{9}\log^2\frac{\mu_Q}{m_Q}\,. \tag{37}$$

At NNNLO, we find

$$\begin{aligned}
M_{gg}^{(3)} &= \frac{564731}{41472} - \frac{2821}{288}\log\frac{\mu_Q}{m_Q} + \frac{3}{16}\log^2\frac{\mu_Q}{m_Q} - \frac{1}{27}\log^3\frac{\mu_Q}{m_Q} - \frac{82043}{9216}\zeta(3)\\
&\quad + n_f\left[-\frac{2633}{10368} + \frac{67}{96}\log\frac{\mu_Q}{m_Q} - \frac{1}{3}\log^2\frac{\mu_Q}{m_Q}\right],\\
M_{qg}^{(2)} &= -\frac{89}{54} + \frac{20}{9}\log\frac{\mu_Q}{m_Q} - \frac{8}{3}\log^2\frac{\mu_Q}{m_Q}\,.
\end{aligned} \tag{38}$$

Conversely, if M is known, the relation in Eq. (29) determines quark matrix elements in the (n_f+1)-flavor theory in terms of those in the n_f-flavor theory, up to power corrections. Employing the results for M_{gQ} and M_{qQ} from Ref. [51], the matrix element for the heavy quark in the (n_f+1)-flavor theory is given by

$$\begin{aligned}
\langle O_Q'^{(0)}\rangle/m_N &= M_{qQ}\lambda + M_{gQ}\frac{2}{\tilde\beta^{(n_f)}}[1-(1-\gamma_m^{(n_f)})\lambda]\\
&= \frac{1}{3\beta_0^{(n_f)}}\left\{2-2\lambda\right\} + \frac{\alpha_s^{(n_f+1)}(\mu_Q)}{\pi}\left(\frac{1}{3\beta_0^{(n_f)}}\right)^2\left\{\frac{57}{2} - \frac{321\lambda}{2} + 8n_f\right\}
\end{aligned}$$

[12] In the notation of Ref. [51], $M_{gQ} = C_1$ and $M_{qQ} = C_2 - 1$. Scheme dependence of C_1 and C_2 enters at $\mathcal{O}(\alpha_s^3)$.

$$+\left(\frac{\alpha_s^{(n_f+1)}(\mu_Q)}{\pi}\right)^2\left(\frac{1}{3\beta_0^{(n_f)}}\right)^3\left\{\frac{9145}{8}-\frac{90985\lambda}{8}+\frac{19437}{4}\log\frac{\mu_Q}{m_Q}-\frac{109461\lambda}{4}\log\frac{\mu_Q}{m_Q}\right.$$
$$+n_f\left[\frac{374}{3}+\frac{1420\lambda}{3}+756\log\frac{\mu_Q}{m_Q}+3424\lambda\log\frac{\mu_Q}{m_Q}\right]+n_f^2\left[\frac{7661}{144}-\frac{7469\lambda}{144}\right.$$
$$\left.\left.-\frac{455}{3}\log\frac{\mu_Q}{m_Q}-107\lambda\log\frac{\mu_Q}{m_Q}\right]+n_f^3\left[-\frac{77}{72}+\frac{77\lambda}{72}+\frac{16}{3}\log\frac{\mu_Q}{m_Q}\right]\right\}$$
$$+\left(\frac{\alpha_s^{(n_f+1)}(\mu_Q)}{\pi}\right)^3\left(\frac{1}{3\beta_0^{(n_f)}}\right)^4\langle O_Q^{\prime(0)}\rangle_4+\mathcal{O}(\alpha_s^4)\,, \tag{39}$$

where the scale independent quantity $\lambda \equiv \sum_{q=u,d,s,\ldots}\langle O_q^{(0)}\rangle/m_N$ is the sum of light quark scalar matrix elements in the n_f-flavor theory. The result for $\langle O_Q^{\prime(0)}\rangle_4$ can be found in Appendix B. The functions M_{gQ}, M_{qQ} and the relation between $\alpha_s^{(n_f)}(\mu_Q)$ and $\alpha_s^{(n_f+1)}(\mu_Q)$ are also given in Ref. [51] in terms of the pole mass $m_Q^{(\mathrm{pole})}$, and we check that the resulting matrix element $\langle O_Q^{\prime(0)}\rangle$ is consistent with the relation between m_Q and $m_Q^{(\mathrm{pole})}$ given in Ref. [53].

In Sec. 4, we employ this solution to determine the charm scalar matrix element in the 4-flavor theory in terms of light quark scalar matrix elements measured in 3-flavor lattice QCD. We note that the solutions for M_{qq}, $M_{qq'}$ and M_{gq}, imply the equality of light quark scalar nucleon matrix elements in n_f and n_f+1 flavor theories, up to power corrections,

$$\langle O_q^{\prime(0)}\rangle = \langle O_q^{(0)}\rangle + \mathcal{O}(1/m_Q)\,. \tag{40}$$

Further iteration of these solutions determine scalar matrix elements for the bottom and top quarks.

Our result in Eq. (39) disagrees with the result given in Eq. (B9) in Appendix B of Ref. [54]. In particular, the expression for $\langle O_Q^{\prime(0)}\rangle$ given there implies results for M_{gQ} and M_{qQ} that do not agree with those of Ref. [51] beyond leading order. Moreover, employing the result of Ref. [54] in (34) yields the NLO result for arbitrary μ_Q, $M_{gg}=1+\mathcal{O}(\alpha_s^2)$, in disagreement with Ref. [50]. A complete comparison cannot be made since Ref. [54] does not specify a scheme choice for the heavy quark mass, however M_{gQ} at $\mathcal{O}(\alpha_s^2)$, M_{qQ} at $\mathcal{O}(\alpha_s^3)$ and M_{gg} at $\mathcal{O}(\alpha_s)$ are independent of scheme choice. In terms of the matrix element $\langle O_Q^{\prime(0)}\rangle$, the $\mathcal{O}(\alpha_s)$ piece differs by terms proportional to $\log\frac{\mu_Q}{m_Q}$, while the $\mathcal{O}(\alpha_s^2)$, $\mathcal{O}(\alpha_s^3)$ and $\mathcal{O}(\alpha_s^4)$ pieces disagree even at $\mu_Q=m_Q$. The scalar matrix element for a heavy quark was also determined in Ref. [55], however a clear comparison is not straightforward given the details presented there.[13]

3.6 Low-energy coefficients

To summarize, the matrices R given in Table 5 of Sec. 3.3 and M given in Table 6 of Secs. 3.4 and 3.5 completely specify the mapping of coefficients down to low energies. For example, coefficients $c_i(\mu_t)$ defined in the five-flavor theory at scale μ_t are mapped onto coefficients $c_i(\mu_0)$ defined in the 3-flavor theory at scale μ_0 as

$$c_j(\mu_0) = R_{jk}(\mu_0,\mu_c)M_{kl}(\mu_c)R_{lm}(\mu_c,\mu_b)M_{mn}(\mu_b)R_{ni}(\mu_b,\mu_t)c_i(\mu_t)\,. \tag{41}$$

Having determined these coefficients, we proceed to analyze the relevant nucleon matrix elements.

[13] The result in Ref. [55] has the scaling $\langle O_Q^{(0)}\rangle \propto (1-\lambda)$, which does not agree with Eq. (39) and Ref. [54].

q	$F_1^{(p,q)}(0)$	$F_2^{(p,q)}(0)$	$F_2^{(p,q)}(0)$
u	2	1.62(2)	1.65(7)
d	1	−2.08(2)	−2.05(7)
s	0	−0.046(19)	−0.017(74)

Table 7: Scale independent vector form factors for the proton at $q^2 = 0$ for light quark flavors u, d, s. For $F_2^{(p,q)}(0)$ we present values in the second and third column employing μ_s from Refs. [56] and [57], respectively. The uncertainties are combined in quadrature and symmetrized. The vector form factors for the neutron follow from approximate isospin symmetry expressed in (42).

4 Hadronic matrix elements

Having determined the structure of the effective theory in terms of quark and gluon degrees of freedom in $n_f = 3$ (or $n_f = 4$) flavor QCD, we may evaluate the resulting nuclear matrix elements at a renormalization scale $\mu \sim 1-2\,\text{GeV}$. As a natural handoff point to nuclear modeling, the subsequent section identifies these matrix elements with matching coefficients of a nucleon-level effective theory.

In this section, we use nonrelativistic normalization $\bar{u}(k)u(k) = m_N/E_{\boldsymbol{k}}$ for nucleon spinors. For the matrix elements of the vector, axial-vector, C-even spin-two and C-odd spin-two operators, we employ approximate isospin symmetry, neglecting small corrections proportional to $m_u - m_d$ and α, to relate proton and neutron matrix elements as

$$\langle p|O_u|p\rangle = \langle n|O_d|n\rangle\,, \quad \langle p|O_d|p\rangle = \langle n|O_u|n\rangle\,, \quad \langle p|O_s|p\rangle = \langle n|O_s|n\rangle\,. \tag{42}$$

The proton and neutron tensor charges $t_{q,N}$ defined in Eqs. (52) and (53) are also related by (42), while the matrix element of the tensor current T_q itself requires the appropriate quark mass factor. For the scalar and pseudoscalar matrix elements, we tabulate both the proton and neutron form factors. The corrections to zero momentum transfer ($q^2 \to 0$) are suppressed in the nonrelativistic regime of typical WIMP-nucleon scattering processes. We discuss the these corrections in Appendix B.

4.1 Vector current matrix elements

For vector currents we parametrize matrix elements as

$$\langle N(k')|V_\mu^{(q)}|N(k)\rangle \equiv \bar{u}(k')\left[F_1^{(N,q)}(q^2)\gamma_\mu + \frac{i}{2m_N}F_2^{(N,q)}(q^2)\sigma_{\mu\nu}q^\nu\right]u(k)\,, \tag{43}$$

where $q \equiv k' - k$ and N denotes a proton (p) or neutron (n). The Dirac $F_1^{(N,q)}$ form factors are normalized according to quark content. The Pauli form factors $F_2^{(N,q)}(0)$ give the contribution of quark flavor q to the nucleon anomalous magnetic moment a_N,

$$\begin{aligned} a_p \equiv F_2^{(p)}(0) &= \frac{2}{3}F_2^{(p,u)}(0) - \frac{1}{3}F_2^{(p,d)}(0) - \frac{1}{3}F_2^{(p,s)}(0)\,, \\ a_n \equiv F_2^{(n)}(0) &= \frac{2}{3}F_2^{(n,u)}(0) - \frac{1}{3}F_2^{(n,d)}(0) - \frac{1}{3}F_2^{(n,s)}(0)\,, \end{aligned} \tag{44}$$

where $a_p \approx 1.79$ and $a_n \approx -1.91$. A phenomenological analysis employing lattice data [56] and a direct lattice simulation with $n_f = 2+1$ dynamical quarks [57] support a small value for the strange

μ (GeV)	$F_A^{(p,u)}(0)$	$F_A^{(p,d)}(0)$	$F_A^{(p,s)}(0)$	Ref
1-2	0.75(8)	-0.51(8)	-0.15(8)	[59]
1	0.80(3)	-0.46(4)	-0.12(8)	[60]
2	0.79(5)	-0.46(5)	-0.13(10)	[60]

Table 8: Axial-vector form factors for the proton at $q^2 = 0$ for light quark flavors u, d, s. The form factors in the first line are extracted from the non-singlet and singlet form factors in Eq. (49), while the form factors in the second and third lines are from the NNPDF parameterization [60] at indicated values of μ. The axial-vector form factors for the neutron follow from approximate isospin symmetry expressed in (42).

contribution to the proton magnetic moment [58],

$$F_2^{(p,s)}(0) \equiv \mu_s = \begin{cases} -0.046(19) & [56] \\ -0.017(25)(70) & [57] \end{cases} . \tag{45}$$

Equations (44) and (45), together with the approximate isospin symmetry expressed in (42), yield $F_2^{(p,u)}(0) = 2a_p + a_n + \mu_s$ and $F_2^{(p,d)}(0) = a_p + 2a_n + \mu_s$. Numerical values for the proton form factors are collected in Table 7. The q^2 dependence of $F_1^{(p,q)}(q^2)$ is described in Appendix B. Following from (42), the neutron form factors for $i = 1, 2$ are

$$F_i^{(n,d)} = F_i^{(p,u)} , \quad F_i^{(n,u)} = F_i^{(p,d)} , \quad F_i^{(n,s)} = F_i^{(p,s)} . \tag{46}$$

4.2 Axial-vector current matrix elements

For the axial-vector currents we parametrize matrix elements as

$$\langle N(k')|A_\mu^{(q)}|N(k)\rangle \equiv \bar{u}^{(N)}(k') \left[F_A^{(N,q)}(q^2)\gamma_\mu\gamma_5 + \frac{1}{2m_N} F_{P'}^{(N,q)}(q^2)\gamma_5 q_\mu \right] u^{(N)}(k) , \tag{47}$$

and it is convenient to consider flavor non-singlet ($A^{(3)}$, $A^{(8)}$) and flavor singlet ($A^{(0)}$) linear combinations,

$$\begin{aligned} A_\mu^{(3)} &= \bar{Q}\gamma_\mu\gamma_5 T^3 Q = \frac{1}{2}\left[\bar{u}\gamma_\mu\gamma_5 u - \bar{d}\gamma_\mu\gamma_5 d\right] , \\ A_\mu^{(8)} &= \bar{Q}\gamma_\mu\gamma_5 T^8 Q = \frac{1}{2\sqrt{3}}\left[\bar{u}\gamma_\mu\gamma_5 u + \bar{d}\gamma_\mu\gamma_5 d - 2\bar{s}\gamma_\mu\gamma_5 s\right] , \\ A_\mu^{(0)} &= \frac{1}{3}\bar{Q}\gamma_\mu\gamma_5 Q = \frac{1}{3}\left[\bar{u}\gamma_\mu\gamma_5 u + \bar{d}\gamma_\mu\gamma_5 d + \bar{s}\gamma_\mu\gamma_5 s\right] . \end{aligned} \tag{48}$$

In the limit of $SU(3)$ flavor symmetry, the $q^2 = 0$ limit for these matrix elements can be extracted from hyperon semileptonic decay and νp scattering [59],

$$F_A^{(p,3)}(0) = \frac{(F+D)}{2} = 0.63(2) , \quad F_A^{(p,8)}(0) = \frac{(3F-D)}{2\sqrt{3}} = 0.16(2) , \quad F_A^{(p,0)}(0\,,\mu) = 0.03(8) , \tag{49}$$

μ (GeV)	$t_{u,p}(\mu)$	$t_{d,p}(\mu)$	$t_{s,p}(\mu)$	Ref
-	4/3	-1/3	0	-
1.0	0.88(6)	-0.24(5)	-0.05(3)	-
1.4	0.84(6)	-0.23(5)	-0.05(3)	[63]
2.0	0.81(6)	-0.22(5)	-0.05(3)	-

Table 9: Tensor charges from a nonrelativistic quark model (μ unspecified) and the lattice measurement in Ref. [63] at $\mu \approx 1.4\,\text{GeV}$ for a proton. The values at $\mu = 1, 2\,\text{GeV}$ are obtained by scale evolution of the tensor charges from $\mu = 1.4\,\text{GeV}$. The tensor charges for the neutron follow from approximate isospin symmetry expressed in (42).

where $D = 0.80(2)$ and $F = 0.45(2)$. The non-singlet currents are scale independent but the flavor singlet current has weak scale dependence governed by the anomalous dimension $\gamma_A^{(\text{singlet})}$ in Table 4, corresponding to the solution $R_A^{(\text{singlet})}$ in Table 5. In particular, with $n_f = 3$, running from $\mu = 2\,\text{GeV}$ to $\mu = 1\,\text{GeV}$ gives a factor of $R_A^{(\text{singlet})}(1\,\text{GeV}, 2\,\text{GeV}) = 0.96$, and we may thus consider $F_A^{(p,0)}$ in Eq. (49) to be evaluated at $\mu = 1 - 2\,\text{GeV}$. The first line of Table 8 lists the matrix elements of definite quark flavor from solving (48) and employing numerical values in (49).

The $q^2 = 0$ limit of these form factors may also be constrained by observables of polarized deep inelastic scattering, via

$$F_A^{(p,q)}(0) = \int_0^1 dx \left[\Delta q(x,\mu) + \Delta\bar{q}(x,\mu)\right], \tag{50}$$

where $\Delta q(x,\mu)$ is the quark helicity distribution evaluated at scale μ. Numerical values for these matrix elements extracted from the NNPDF collaboration's parameterization of Δq in Ref. [60] are listed in Table 8, showing a negligible scale dependence. Results from lattice calculations [61, 62] are numerically similar. The q^2 dependence of $F_A^{(p,a)}$ is described in Appendix B. Following from (42), the neutron form factors are

$$F_A^{(n,d)} = F_A^{(p,u)}, \quad F_A^{(n,u)} = F_A^{(p,d)}, \quad F_A^{(n,s)} = F_A^{(p,s)}. \tag{51}$$

The terms parametrized by induced pseudoscalar form factors $F_{P'}$ in (47) are suppressed by two powers of $|\boldsymbol{k}|/m_N$, and lead to numerically small contributions in typical WIMP-nucleus scattering processes. For completeness we describe the leading contributions to these form factors in Appendix B.

4.3 Antisymmetric tensor current matrix element

For the antisymmetric tensor currents, we parametrize the matrix element as

$$\frac{E_{\boldsymbol{k}}}{m_N}\langle N(k)|T_{\mu\nu}^{(q)}|N(k)\rangle \equiv \frac{2}{m_N} s^{[\mu}k^{\nu]} m_q(\mu) t_{q,N}(\mu), \tag{52}$$

where $s^\mu = -(E_{\boldsymbol{k}}/2m_N^2)\epsilon^{\mu\nu\rho\sigma}k_\nu\bar{u}(k)\sigma_{\rho\sigma}u(k)$ is the covariant spin vector satisfying $k^\mu s_\mu = 0$ and $s^2 = -1$. In terms of structure functions appearing in polarized deep inelastic scattering, the tensor charges are given as

$$t_{q,N}(\mu) = \int_{-1}^1 dx\, \delta q_N(x,\mu). \tag{53}$$

The functions $\delta q(x,\mu)$ are not yet well constrained experimentally. Table 9 lists values for the proton tensor charges $t_{q,p}$ from a nonrelativistic quark model with $SU(6)$ spin flavor symmetry and from a lattice measurement [63]. Other estimates of $t_{u,p}$, $t_{d,p}$ or $t_{u,p}-t_{d,p}$ have been obtained using lattice QCD methods [64, 65, 66], QCD sum rules [67], modeling [68, 69] and semi-inclusive deep inelastic scattering data [70].

The tensor charges at $\mu = 1,\, 2$ GeV in Table 9 are obtained by scale evolution of the tensor charges at $\mu = 1.4$ GeV using the anomalous dimension $\gamma_T - \gamma_m$ with γ_T given in Table 4 and γ_m the quark mass anomalous dimension given in Appendix A. Together with $m_q(\mu)$, e.g., taken from the PDG [71] or Ref. [72], the tensor charges in Table 9 specify the matrix element of the antisymmetric tensor current $T_q^{\mu\nu}$. Following from (42), the neutron tensor charges are

$$t_{d,n} = t_{u,p}\,, \quad t_{u,n} = t_{d,p}\,, \quad t_{s,n} = t_{s,p}\,. \tag{54}$$

4.4 Scalar matrix elements

For the dimension four scalar operators, we restrict attention to forward nucleon matrix elements. Let us define

$$\frac{E_{\boldsymbol{k}}}{m_N}\langle N(k)|O_q^{(0)}|N(k)\rangle \equiv m_N f_{q,N}^{(0)}\,, \quad \frac{-9\alpha_s(\mu)}{8\pi}\frac{E_{\boldsymbol{k}}}{m_N}\langle N(k)|O_g^{(0)}(\mu)|N(k)\rangle \equiv m_N f_{g,N}^{(0)}(\mu)\,, \tag{55}$$

where the appearance of the numerical factor involving $\alpha_s(\mu)$ is purely conventional. The operator matrix elements are not independent, being linked by the sum rule in Eq. (30) as

$$m_N\bar{u}(k)u(k) = (1-\gamma_m)\sum_q \langle N(k)|m_q\bar{q}q|N(k)\rangle + \frac{\tilde{\beta}}{2}\langle N(k)|(G_{\mu\nu}^a)^2|N(k)\rangle\,, \tag{56}$$

ignoring $\mathcal{O}(1/m_N)$ power corrections. Combining (55) and (56) we have

$$f_{g,N}^{(0)} = -\frac{\alpha_s}{4\pi}\frac{9}{\tilde{\beta}}\Big\{1-\big(1-\gamma_m\big)\lambda\Big\} = 1-\lambda+\mathcal{O}(\alpha_s)\,, \tag{57}$$

where $\lambda = \sum_{q=u,d,s} f_{q,N}^{(0)}$, the scale dependence is implicit, and the second equality is obtained by neglecting γ_m and $\mathcal{O}(\alpha_s^2)$ contributions to $\tilde{\beta}$. In Sec. 6, we will see that corrections to the leading order relation are numerically important in the case of electroweak-charged WIMPs.

We may extract the up and down quark scalar nucleon matrix elements from the scale-invariant combinations,

$$\begin{aligned}\Sigma_{\pi N} &= \frac{m_u+m_d}{2}\langle N|(\bar{u}u+\bar{d}d)|N\rangle = 44(13)\,\text{MeV}\,,\\ \Sigma_- &= (m_d-m_u)\langle N|(\bar{u}u-\bar{d}d)|N\rangle = \pm 2(2)\,\text{MeV}\,,\end{aligned} \tag{58}$$

where the upper (lower) sign in Σ_- is for the proton (neutron) [73]. The numerical value for the pion-nucleon sigma term $\Sigma_{\pi N}$ is the lattice result from Ref. [74] with errors symmetrized. For the strange scalar nucleon matrix element, we use the updated lattice result $m_N f_{s,N}^{(0)} = 40 \pm 20\,\text{MeV}$ from Ref. [75], where we assume a conservative 50% uncertainty compared to their estimate of 25%.

For models with identical couplings to up and down quarks, it is sufficient to take as input $m_N\big(f_{u,N}^{(0)} + f_{d,N}^{(0)}\big) = \Sigma_{\pi N} - \Sigma_-/2 \approx \Sigma_{\pi N}$, neglecting the small contribution from Σ_-. For general applications requiring separately the up and down quark scalar matrix elements let us write

$$f_{u,N}^{(0)} = \frac{R_{ud}}{1+R_{ud}}\frac{\Sigma_{\pi N}}{m_N}(1+\xi)\,, \quad f_{d,N}^{(0)} = \frac{1}{1+R_{ud}}\frac{\Sigma_{\pi N}}{m_N}(1-\xi)\,, \quad \xi = \frac{1+R_{ud}}{1-R_{ud}}\frac{\Sigma_-}{2\Sigma_{\pi N}}\,, \tag{59}$$

q	$f^{(0)}_{q,p}$	$f^{(0)}_{q,n}$
u	$0.016(5)(3)(1)$	$0.014(5)(^{+2}_{-3})(1)$
d	$0.029(9)(3)(2)$	$0.034(9)(^{+3}_{-2})(2)$
s	$0.043(21)$	$0.043(21)$

Table 10: Scale independent scalar form factors for the proton and neutron for light quark flavors u, d, s. The first, second and third uncertainties are from $\Sigma_{\pi N}$, m_u/m_d and Σ_-, respectively. As discussed below Eq. (60), the parameterization in Eq. (59) leads to highly correlated uncertainties in $f^{(0)}_{u,N}$ and $f^{(0)}_{d,N}$.

where we employ the quark mass ratios adopted from PDG values [71] (symmetrizing errors),

$$R_{ud} \equiv \frac{m_u}{m_d} = 0.49 \pm 0.13\,, \quad R_{sd} \equiv \frac{m_s}{m_d} = 19.5 \pm 2.5\,. \tag{60}$$

The resulting numerical values for the light quark scalar matrix elements are collected in Table 10. The uncertainties in $f^{(0)}_{u,N}$ and $f^{(0)}_{d,N}$ are highly correlated, and for applications we use Eq. (59), varying the inputs $\Sigma_{\pi N}$, R_{ud} and Σ_- whose uncertainties are taken as uncorrelated. The (subleading) uncertainty from Σ_- may be further reduced by employing the analysis in Ref. [76]. For both proton and neutron, the gluon matrix element $f^{(0)}_{g,N}$ is obtained from the quark matrix elements via the sum rule in Eq. (56).

From the analysis of heavy quark matching conditions in Sec. 3.5, we may determine the scalar matrix elements of heavy quark flavors. For definiteness, let us consider 4-flavor QCD with a heavy charm quark. Denoting quantities in the 4-flavor (3-flavor) theory with (without) a prime, the results in Eqs. (39) and (40) yield

$$\begin{aligned} f^{(0)\prime}_{c,N} &= 0.083 - 0.103\lambda + \mathcal{O}(\alpha_s^4, 1/m_c) = 0.073(3) + \mathcal{O}(\alpha_s^4, 1/m_c)\,, \\ f^{(0)\prime}_{q,N} &= f^{(0)}_{q,N} + \mathcal{O}(1/m_c)\,, \end{aligned} \tag{61}$$

where we use $\lambda \approx \Sigma_{\pi N}/m_N + f^{(0)}_{s,N} = 0.089(26)\,\text{MeV}$, neglecting the small contribution from Σ_-. An expression for $f^{(0)\prime}_{c,N}$ in terms of $\alpha_s'(\mu_c)$ is given in Appendix B; in particular, the $\mathcal{O}(\alpha_s^3)$ term in $f^{(0)\prime}_{c,N}$ employs $\langle O'^{(0)}_Q\rangle_4$ derived in Sec. 3.5. The uncertainty in $f^{(0)\prime}_{c,N}$ is presently dominated by hadronic inputs, and in (61) we neglect the small uncertainty ($< 1\%$) from scale variation of μ_c. Recent lattice measurements of the charm matrix element in Refs. [77] and [78] have determined

$$f^{(0)\prime}_{c,N} = \begin{cases} 0.10(3)\ [77] \\ 0.07(3)\ [78] \end{cases}\,, \tag{62}$$

which are consistent within large errors with (61). As discussed below (39), we find discrepancies with previous determinations of the heavy quark scalar matrix elements [54, 55].[14] Nonetheless, due to a large $\mathcal{O}(30\%)$ uncertainty in λ, the resulting numerical values are consistent. A nonperturbative determination of the charm and light quark matrix elements in 4-flavor lattice QCD would avoid uncertainties associated with the charm scale $\mu_c \sim m_c$, such as $\mathcal{O}(1/m_c)$ power corrections and $\mathcal{O}(\alpha_s)$ perturbative corrections. In Sec. 6, we investigate the evaluation of the spin-independent cross section for heavy electroweak-charged WIMPs in the 4-flavor theory.

[14] In Ref. [75], the result of Ref. [55] was presented with updated inputs.

q	$f^{(0)}_{5q,p}$	Ref. [79]	$f^{(0)}_{5q,n}$	Ref. [79]
u	0.42(8)(1)	0.43	-0.41(8)(1)	-0.42
d	-0.84(8)(3)	-0.84	0.85(8)(3)	0.85
s	-0.48(8)(1)(3)	-0.50	-0.06(8)(1)(3)	-0.08

Table 11: Scale invariant quark pseudoscalar form factors evaluated at $\kappa(0,\mu) = 0$. We list numbers for the proton and neutron obtained from (65) with inputs from (60) and (49), and compare to the values in Table II of Ref. [79]. The first, second and third uncertainties are respectively from R_{ud}, $F_A^{(p,3)}$ and $F_A^{(p,8)}$; negligible uncertainties are not shown.

4.5 Pseudoscalar matrix elements

For the quark and gluon pseudoscalar operators we parametrize the matrix elements as

$$\begin{aligned}
\frac{E_{\boldsymbol{k}}}{m_N}\langle N(k')|O^{(0)}_{5q}|N(k)\rangle &\equiv m_N f^{(0)}_{5q,N}(q^2)\bar{u}(k')i\gamma_5 u(k)\,,\\
\frac{E_{\boldsymbol{k}}}{m_N}\langle N(k')|O^{(0)}_{5g}|N(k)\rangle &\equiv m_N f^{(0)}_{5g,N}(q^2)\bar{u}(k')i\gamma_5 u(k)\,,
\end{aligned} \tag{63}$$

where the quark pseudoscalar operators have been defined independent of renormalization scale, while the gluon operators have a weak scale dependence. The matrix elements in Eq. (63) are related to the matrix elements of the axial vector current through the axial anomaly in Eq. (18). Employing the matrix elements for the non-singlet axial-vector currents in Eq. (49), together with the additional definition,

$$\sum_{q=u,d,s}\langle N(k')|\bar{q}i\gamma_5 q|N(k)\rangle \equiv \kappa(q^2,\mu)\bar{u}(k')i\gamma_5 u(k)\,, \tag{64}$$

we find the following quark pseudoscalar form factors at $q^2 = 0$:

$$\begin{aligned}
f^{(0)}_{5u,p}(0) &= \frac{R_{ud}\Big(\sqrt{3}F_A^{(p,8)}(0) + \big[1+2R_{sd}\big]F_A^{(p,3)}(0)\Big)}{R_{sd}+R_{ud}+R_{sd}R_{ud}} + \omega\,,\\
f^{(0)}_{5d,p}(0) &= \frac{\sqrt{3}F_A^{(p,8)}(0)R_{ud} - \big[R_{ud}+2R_{sd}\big]F_A^{(p,3)}(0)}{R_{sd}+R_{ud}+R_{sd}R_{ud}} + \omega\,,\\
f^{(0)}_{5s,p}(0) &= \frac{R_{sd}\Big(-\sqrt{3}\big[1+R_{ud}\big]F_A^{(p,8)}(0) - \big[1-R_{ud}\big]F_A^{(p,3)}(0)\Big)}{R_{sd}+R_{ud}+R_{sd}R_{ud}} + \omega\,,
\end{aligned} \tag{65}$$

where the quark mass ratios $R_{qq'} = m_q/m_{q'}$ are given in (60) and ω is the scale independent quantity,

$$\omega = \frac{\kappa(0,\mu)m_d(\mu)R_{sd}R_{ud}}{m_N\Big(R_{sd}+R_{ud}+R_{sd}R_{ud}\Big)}\,. \tag{66}$$

In the absence of better information on the quantity $\kappa(q^2,\mu)$, we list numerical values for the quark form factors in Table 11 setting $\kappa(0,\mu) = 0$, as motivated by large N_c arguments [79]. This standard

μ (GeV)	$f^{(2)}_{u,p}(\mu)$	$f^{(2)}_{d,p}(\mu)$	$f^{(2)}_{s,p}(\mu)$	$f^{(2)}_{c,p}(\mu)$	$f^{(2)}_{b,p}(\mu)$	$f^{(2)}_{g,p}(\mu)$
1	0.404(9)	0.217(8)	0.024(4)	-	-	0.356(29)
1.2	0.383(8)	0.208(8)	0.027(4)	-	-	0.381(25)
1.4	0.370(8)	0.202(7)	0.030(4)	-	-	0.398(23)
2	0.346(7)	0.192(6)	0.034(3)	-	-	0.419(19)
$80.4/\sqrt{2}$	0.260(4)	0.158(4)	0.053(2)	0.036(1)	0.0219(4)	0.470(8)
100	0.253(4)	0.156(4)	0.055(2)	0.038(1)	0.0246(5)	0.472(8)
$172\sqrt{2}$	0.244(4)	0.152(3)	0.057(2)	0.042(1)	0.028(1)	0.476(7)

Table 12: Form factors for C-even spin-two operators derived from MSTW analysis [80] at different values of μ. The neutron form factors follow from approximate isospin symmetry expressed in (42).

ansatz should be revisited if observables are found to be sensitive to nonzero ω. The matrix element for the pseudoscalar gluon operator may then be obtained through Eq. (18),

$$f^{(0)}_{5g,N}(0) = \frac{16\pi}{\alpha_s(\mu)}\left[\frac{1}{3}\sum_q f^{(0)}_{5q,N}(0) - F_A^{(p,0)}(0,\mu)\right]. \tag{67}$$

As discussed below (49), the scale dependence from the singlet axial-vector form factor $F_A^{(p,0)}(0,\mu)$ is weak. The neutron form factors presented in Table. 11 were obtained using approximate isospin symmetry for the axial-vector currents, i.e., taking $F_A^{(n,3)} = -F_A^{(p,3)}$ in (65).

4.6 C-even spin-two matrix elements

For C-even spin-two operators, the forward matrix elements are parametrized as

$$\begin{aligned}
\frac{E_{\boldsymbol{k}}}{m_N}\langle N(k)|O_q^{(2)\mu\nu}(\mu)|N(k)\rangle &\equiv \frac{1}{m_N}\left(k^\mu k^\nu - \frac{g^{\mu\nu}}{4}m_N^2\right) f^{(2)}_{q,N}(\mu)\,,\\
\frac{E_{\boldsymbol{k}}}{m_N}\langle N(k)|O_g^{(2)\mu\nu}(\mu)|N(k)\rangle &\equiv \frac{1}{m_N}\left(k^\mu k^\nu - \frac{g^{\mu\nu}}{4}m_N^2\right) f^{(2)}_{g,N}(\mu)\,,
\end{aligned} \tag{68}$$

and are identified as moments of parton distribution functions constrained in unpolarized deep inelastic scattering,

$$f^{(2)}_{q,p}(\mu) = \int_0^1 dx\, x[q(x,\mu) + \bar{q}(x,\mu)]\,, \tag{69}$$

where $q(x,\mu)$ is the parton distribution function evaluated at scale μ. Neglecting power corrections, the sum of spin two operators is identified as the traceless part of the QCD energy momentum tensor,

$$\sum_{q=u,d,s} f^{(2)}_{q,p}(\mu) + f^{(2)}_{g,p}(\mu) = 1\,. \tag{70}$$

Table 12 lists coefficient values for renormalization scales $\mu = 1, 1.2, 1.4, 2, m_W/\sqrt{2}, 100, m_t\sqrt{2}$ GeV using the parameterization and analysis of MSTW [80]. Following from (42), the neutron form factors are

$$f^{(2)}_{u,n} = f^{(2)}_{d,p}\,, \quad f^{(2)}_{d,n} = f^{(2)}_{u,p}\,, \quad f^{(2)}_{s,n} = f^{(2)}_{s,p}\,. \tag{71}$$

4.7 C odd, spin two matrix elements

μ (GeV)	$f^{(2)}_{5u,p}(\mu)$	$f^{(2)}_{5d,p}(\mu)$	$f^{(2)}_{5s,p}(\mu)$
1.0	0.186(7)	-0.069(8)	-0.007(6)
1.2	0.175(6)	-0.065(7)	-0.006(6)
1.4	0.167(6)	-0.062(7)	-0.006(5)
2.0	0.154(5)	-0.056(6)	-0.005(5)

Table 13: Form factors for C-odd spin-two operators derived from NNPDF analysis [60] at different values of μ. The neutron form factors follow from approximate isospin symmetry expressed in (42).

For C-odd spin-two operators, we parametrize the matrix elements as [81]

$$\frac{E_{\boldsymbol{k}}}{m_N}\langle N(k)|O^{(2)\mu\nu}_{5q}(\mu)|N(k)\rangle \equiv s^{\{\mu}k^{\nu\}}f^{(2)}_{5q,N}(\mu)\,, \tag{72}$$

where s^μ is the nucleon spin defined below (52). The coefficients are moments of polarized structure functions

$$f^{(2)}_{5q,N}(\mu) = \int_0^1 dx\, x[\Delta q(x,\mu) + \Delta\bar{q}(x,\mu)]\,. \tag{73}$$

Table 13 lists coefficient values for the proton, at renormalization scales $\mu = 1, 1.2, 1.4, 2$ GeV using the parameterization and analysis of NNPDF [60]. Following from (42), the neutron form factors are

$$f^{(2)}_{5u,n} = f^{(2)}_{5d,p}\,, \quad f^{(2)}_{5d,n} = f^{(2)}_{5u,p}\,, \quad f^{(2)}_{5s,n} = f^{(2)}_{5s,p}\,. \tag{74}$$

5 Nucleon level effective theory

At energy scales much lower than $\Lambda_{\rm QCD}, m_\pi$, it is useful to employ an effective description in terms of nucleon degrees of freedom. We consider WIMP-hadron interactions given either through electromagnetic couplings, or by contact operators with contractions of Lorentz vector indices (perhaps including heavy-particle reference vectors v_μ) and the QCD operators of the previous section. The heavy nucleon lagrangian is given by

$$\mathcal{L}_N = \bar{N}_u\Big\{iu\cdot D - \frac{D_\perp^2}{2m_N} + \dots\Big\}N_u\,, \tag{75}$$

where $D_\mu = \partial_\mu - ieQA_\mu$ is the electromagnetic gauge covariant derivative, and we have introduced the timelike invariant vector u^μ for the nucleon N_u, in addition to v^μ for the WIMP.

5.1 Matching conditions in single nucleon sector

We begin by constructing the heavy particle representation of the nucleon. For the SM current, at $d = 2$ we require the representation for the photon $F_{\mu\nu}$, which is trivial. At $d = 3$ we have the vector and axial-vector currents which match to

$$u_\mu V_q^\mu = \Big[F_1^{(q)}(0)\Big]\bar{N}_uN_u + \frac{1}{m_N^2}\Big\{\Big[-\frac{1}{8}F_1^{(q)}(0) - m_N^2F_1^{(q)\prime}(0) - \frac{1}{4}F_2^{(q)}(0)\Big]\partial_\perp^2\big(\bar{N}_uN_u\big)$$

$$
\begin{aligned}
&+\Big[-\frac{1}{4}F_1^{(q)}(0)-\frac{1}{2}F_2^{(q)}(0)\Big]i\bar N_u\partial_\perp^\mu\overleftarrow{\partial}_\perp^{\,\nu}\sigma_{\perp\mu\nu}N_u\Big\}+\mathcal{O}(1/m_N^4)\,,\\
V_{q\perp}^\mu&=\frac{1}{m_N}\Big\{\Big[\frac{1}{2}F_1^{(q)}(0)\Big]i\bar N_u\overleftrightarrow{\partial}_\perp^{\,\mu}N_u+\Big[\frac{1}{2}F_1^{(q)}(0)+\frac{1}{2}F_2^{(q)}(0)\Big]\partial_{\perp\nu}\big(\bar N_u\sigma_\perp^{\mu\nu}N_u\big)\Big\}+\mathcal{O}(1/m_N^3)\,,\\
u_\mu A_q^\mu&=\frac{1}{m_N}\Big\{\Big[-\frac{1}{4}F_A^{(q)}(0)\Big]i\epsilon^{\mu\nu\rho\sigma}u_\mu\bar N_u\overleftrightarrow{\partial}_{\perp\nu}\sigma_{\perp\rho\sigma}N_u\Big\}+\mathcal{O}(1/m_N^3)\,,\\
A_{q\perp}^\mu&=\Big[-\frac{1}{2}F_A^{(q)}(0)\Big]\epsilon^{\mu\nu\rho\sigma}u_\nu\bar N_u\sigma_{\perp\rho\sigma}N_u\\
&+\frac{1}{m_N^2}\Big\{\Big[\frac{1}{8}F_A^{(q)}(0)+m_N^2F_A^{(q)\prime}(0)\Big]\epsilon^{\mu\nu\rho\sigma}u_\nu\bar N_u\overleftarrow{\partial}_\perp^{\,\alpha}\partial_{\perp\alpha}\sigma_{\perp\rho\sigma}N_u\\
&+\Big[-\frac{1}{16}F_A^{(q)}(0)+\frac{1}{2}m_N^2F_A^{(q)\prime}(0)\Big]\epsilon^{\mu\nu\rho\sigma}u_\nu\bar N_u\big(\overleftarrow{\partial}^{\,2}+\partial_\perp^2\big)\sigma_{\perp\rho\sigma}N_u\\
&+\Big[-\frac{1}{8}F_{P'}^{(q)}(0)\Big]\epsilon_{\alpha\beta\gamma\delta}u^\gamma\bar N_u\big(\partial_\perp^\mu\partial_\perp^\alpha+\overleftarrow{\partial}_\perp^{\,\mu}\overleftarrow{\partial}_\perp^{\,\alpha}\big)\sigma_\perp^{\beta\delta}N_u\\
&+\Big[-\frac{1}{8}F_A^{(q)}(0)-\frac{1}{8}F_{P'}^{(q)}(0)\Big]\epsilon_{\alpha\beta\gamma\delta}u^\gamma\bar N_u\big(\partial_\perp^\mu\overleftarrow{\partial}_\perp^{\,\alpha}+\overleftarrow{\partial}_\perp^{\,\mu}\partial_\perp^\alpha\big)\sigma_\perp^{\beta\delta}N_u\\
&+\Big[-\frac{1}{4}F_A^{(q)}(0)\Big]i\epsilon^{\mu\nu\alpha\beta}u_\nu\bar N_u\partial_{\perp\alpha}\overleftarrow{\partial}_{\perp\beta}N_u\Big\}+\mathcal{O}(1/m_N^4)\,,
\end{aligned}
\tag{76}
$$

where we have expressed the matching coefficients (the quantities in square brackets) in terms of the form factors of the previous section, and decomposed the currents into components along and perpendicular to u^μ. At $d=4$, we work through $\mathcal{O}(1/m_N)$, i.e., first derivative order, and have the antisymmetric tensor currents, the scalar and pseudoscalar operators, and the C-even and C-odd spin-two operators. Employing the notation in Table 2 and expressing results in terms of matrix elements of the previous section, the matching conditions are

$$
\begin{aligned}
T_q^{\mu\nu}&=m_N\Big[\Big(\frac{m_q t_q}{m_N}\Big)\epsilon^{\alpha\beta\gamma[\mu}u^{\nu]}u_\alpha\bar N\sigma_{\beta\gamma}^\perp N+\mathcal{O}(1/m_N^2)\Big]\,,\\
O_q^{(0)}&=m_N\Big[f_q^{(0)}\bar N_uN_u+\mathcal{O}(1/m_N^2)\Big]\,,\\
O_g^{(0)}&=m_N\Big[\Big(\frac{-8\pi}{9\alpha_s}\Big)f_g^{(0)}\bar N_uN_u+\mathcal{O}(1/m_N^2)\Big]\,,\\
O_{5q,5g}^{(0)}&=\frac{1}{4}f_{5q,5g}^{(0)}\epsilon^{\mu\nu\rho\sigma}u_\mu\partial_{\perp\nu}(\bar N\sigma_{\rho\sigma}^\perp N)+\mathcal{O}(1/m_N^2)\,,\\
u_\mu u_\nu O_{q,g}^{(2)\mu\nu}&=m_N\Big[\frac{3}{4}f_{q,g}^{(2)}\bar N_uN_u+\mathcal{O}(1/m_N^2)\Big]\,,\\
O_{5q}^{(2)\mu\nu}&=m_N\Big[\frac{1}{2}f_{5q}^{(2)}\epsilon^{\alpha\beta\gamma\{\mu}u^{\nu\}}u_\alpha\bar N\sigma_{\beta\gamma}^\perp N+\mathcal{O}(1/m_N^2)\Big]\,,
\end{aligned}
\tag{77}
$$

where the subscript label N on form factors has been suppressed.

5.2 Nucleon effective theory for light mediators

The forgoing analysis, with additional matching onto multinucleon operators, provides a general framework for WIMP-nucleus scattering in the case where all new states in the dark sector have mass $\gg \Lambda_{\rm QCD}$, such that below this scale, a complete description is possible in terms of a systematic expansion of operators in $n_f = 3$ flavor QCD. Subsequent matching onto nucleon operators is given simply by evaluating the necessary form factors, whose low-q^2 behavior may be determined by lattice QCD, chiral perturbation theory or other nonperturbative methods.

For completeness let us consider a more general situation allowing for light degrees of freedom, with mass only assumed large compared to a typical WIMP-nucleon momentum transfer.[15] We assume that all new states of the dark sector are integrated out, and consider the resulting basis of operators in the one-nucleon sector. Specializing to the choice $v^\mu = u^\mu = (1,0,0,0)$, and neglecting electromagnetic interactions, the kinetic terms may be written,

$$\mathcal{L}_N = N^\dagger \left\{ i\partial_t + \frac{\boldsymbol{\partial}^2}{2m_N} + \dots \right\} N\,, \quad \mathcal{L}_\chi = \chi^\dagger \left\{ i\partial_t + \frac{\boldsymbol{\partial}^2}{2m_\chi} + \dots \right\} \chi\,, \tag{78}$$

where N and χ denote the nonrelativistic nucleon and WIMP fields, respectively. For interactions even under P and T, we find through dimension eight the operators [36, 82],

$$\begin{aligned}
\mathcal{L}_{N\chi,PT} = \frac{1}{m_N^2}\Big\{ & d_1 N^\dagger \sigma^i N\ \chi^\dagger \sigma^i \chi + d_2 N^\dagger N\ \chi^\dagger \chi \Big\} + \frac{1}{m_N^4}\Big\{ d_3 N^\dagger \partial_+^i N\ \chi^\dagger \partial_+^i \chi + d_4 N^\dagger \partial_-^i N\ \chi^\dagger \partial_-^i \chi \\
& + d_5 N^\dagger (\boldsymbol{\partial}^2 + \overleftarrow{\boldsymbol{\partial}}^2) N\ \chi^\dagger \chi + d_6 N^\dagger N\ \chi^\dagger (\boldsymbol{\partial}^2 + \overleftarrow{\boldsymbol{\partial}}^2) \chi + i d_8 \epsilon^{ijk} N^\dagger \sigma^i \partial_-^j N\ \chi^\dagger \partial_+^k \chi \\
& + i d_9 \epsilon^{ijk} N^\dagger \sigma^i \partial_+^j N\ \chi^\dagger \partial_-^k \chi + i d_{11} \epsilon^{ijk} N^\dagger \partial_+^k N\ \chi^\dagger \sigma^i \partial_-^j \chi + i d_{12} \epsilon^{ijk} N^\dagger \partial_-^k N\ \chi^\dagger \sigma^i \partial_+^j \chi \\
& + d_{13} N^\dagger \sigma^i \partial_+^j N\ \chi^\dagger \sigma^i \partial_+^j \chi + d_{14} N^\dagger \sigma^i \partial_-^j N\ \chi^\dagger \sigma^i \partial_-^j \chi + d_{15} N^\dagger \boldsymbol{\sigma}\cdot\boldsymbol{\partial}_+ N\ \chi^\dagger \boldsymbol{\sigma}\cdot\boldsymbol{\partial}_+ \chi \\
& + d_{16} N^\dagger \boldsymbol{\sigma}\cdot\boldsymbol{\partial}_- N\ \chi^\dagger \boldsymbol{\sigma}\cdot\boldsymbol{\partial}_- \chi + d_{17} N^\dagger \sigma^i \partial_-^j N\ \chi^\dagger \sigma^j \partial_-^i \chi \\
& + d_{18} N^\dagger \sigma^i (\boldsymbol{\partial}^2 + \overleftarrow{\boldsymbol{\partial}}^2) N\ \chi^\dagger \sigma^i \chi + d_{19} N^\dagger \sigma^i (\partial^i \partial^j + \overleftarrow{\partial}^j \overleftarrow{\partial}^i) N\ \chi^\dagger \sigma^j \chi \\
& + d_{20} N^\dagger \sigma^i N\ \chi^\dagger \sigma^i (\boldsymbol{\partial}^2 + \overleftarrow{\boldsymbol{\partial}}^2) \chi + d_{21} N^\dagger \sigma^i N\ \chi^\dagger \sigma^j (\partial^i \partial^j + \overleftarrow{\partial}^j \overleftarrow{\partial}^i) \chi \Big\} + \mathcal{O}(1/m_N^6)\,,
\end{aligned} \tag{79}$$

where the naming scheme for Wilson coefficients is from Ref. [36]. (Note in particular that d_i for $i = 7, 10$ are absent in (79), since these operators are proportional to electromagnetic field strength.) Lorentz symmetry is imposed by enforcing invariance under the infinitesimal boost $\boldsymbol{\eta}$ [33, 36]

$$\begin{aligned}
N &\to e^{i m_N \boldsymbol{\eta}\cdot\boldsymbol{x}} \left[1 - \frac{i\boldsymbol{\eta}\cdot\boldsymbol{\partial}}{2m_N} + \frac{\boldsymbol{\sigma}\times\boldsymbol{\eta}\cdot\boldsymbol{\partial}}{4m_N} + \dots \right] N\,, \\
\chi &\to e^{i m_\chi \boldsymbol{\eta}\cdot\boldsymbol{x}} \left[1 - \frac{i\boldsymbol{\eta}\cdot\boldsymbol{\partial}}{2m_\chi} + \frac{\boldsymbol{\sigma}\times\boldsymbol{\eta}\cdot\boldsymbol{\partial}}{4m_\chi} + \dots \right] \chi\,, \\
\partial_t &\to \partial_t - \boldsymbol{\eta}\cdot\boldsymbol{\partial}\,, \quad \boldsymbol{\partial} \to \boldsymbol{\partial} - \boldsymbol{\eta}\partial_t\,.
\end{aligned} \tag{80}$$

This implies the constraints,

$$r d_4 + d_5 = \frac{d_2}{4}\,, \quad d_5 = r^2 d_6\,, \quad 8r(d_8 + r d_9) = -r d_2 + d_1\,, \quad 8r(r d_{11} + d_{12}) = -d_2 + r d_1\,,$$

[15] We are here also assuming that the considered momentum transfers are small enough that pions may be integrated out.

$$rd_{14}+d_{18}=\frac{d_1}{4}\,,\quad d_{18}=r^2d_{20}\,,\quad 2rd_{16}+d_{19}=\frac{d_1}{4}\,,\quad r(d_{16}+d_{17})+d_{19}=0\,,\quad d_{19}=r^2d_{21}\,,\tag{81}$$

where $r=m_\chi/m_N$. With these constraints in place there are ten independent P and T conserving four-fermion operators through dimension eight, including two operators at dimension six.

Operators even under T but odd under P are

$$\begin{aligned}\mathcal{L}_{N\chi,\not P}=\frac{1}{m_N^3}\Big\{&d_1' iN^\dagger\boldsymbol{\sigma}\cdot\boldsymbol{\partial}_- N\chi^\dagger\chi+d_2' iN^\dagger\sigma^i N\chi^\dagger\partial_-^i\chi+d_3' iN^\dagger\partial_-^i N\chi^\dagger\sigma^i\chi+d_4' iN^\dagger N\chi^\dagger\boldsymbol{\sigma}\cdot\boldsymbol{\partial}_-\chi\\&+d_5'\epsilon^{ijk}N^\dagger\sigma^i\partial_+^j N\chi^\dagger\sigma^k\chi\Big\}+\mathcal{O}(1/m_N^5)\,.\end{aligned}\tag{82}$$

Relativistic invariance enforces the constraints

$$d_1'+rd_2'=d_3'+rd_4'=0\,,\tag{83}$$

leaving three independent operators. Operators odd under both P and T are

$$\begin{aligned}\mathcal{L}_{N\chi,\not P\not T}=\frac{1}{m_N^3}\Big\{&f_1' N^\dagger\boldsymbol{\sigma}\cdot\boldsymbol{\partial}_+ N\chi^\dagger\chi+f_2' N^\dagger N\chi^\dagger\boldsymbol{\sigma}\cdot\boldsymbol{\partial}_+\chi+f_3' i\epsilon^{ijk}N^\dagger\sigma^i\partial_-^j N\chi^\dagger\sigma^k\chi\\&+f_4' i\epsilon^{ijk}N^\dagger\sigma^i N\chi^\dagger\sigma^j\partial_-^k\chi\Big\}+\mathcal{O}(1/m_N^5)\,.\end{aligned}\tag{84}$$

Relativistic invariance enforces the constraints

$$f_3'=rf_4'\,,\tag{85}$$

leaving three independent operators. Operators even under P and odd under T are

$$\begin{aligned}\mathcal{L}_{N\chi,\not T}=\frac{1}{m_N^4}\Big\{&if_1 N^\dagger\boldsymbol{\partial}_+\cdot\boldsymbol{\partial}_- N\chi^\dagger\chi+if_2 N^\dagger N\chi^\dagger\boldsymbol{\partial}_+\cdot\boldsymbol{\partial}_-\chi+f_3\epsilon^{ijk}N^\dagger\sigma^i\partial_-^j N\chi^\dagger\partial_-^k\chi\\&+f_4\epsilon^{ijk}N^\dagger\partial_-^i N\chi^\dagger\sigma^j\partial_-^k\chi+if_5 N^\dagger\boldsymbol{\partial}_+\cdot\boldsymbol{\partial}_-\sigma^i N\chi^\dagger\sigma^i\chi+if_6 N^\dagger\boldsymbol{\sigma}\cdot\boldsymbol{\partial}_+\partial_-^i N\chi^\dagger\sigma^i\chi\\&+if_7 N^\dagger\boldsymbol{\sigma}\cdot\boldsymbol{\partial}_- N\chi^\dagger\boldsymbol{\sigma}\cdot\boldsymbol{\partial}_+\chi+if_8 N^\dagger\sigma^i N\chi^\dagger\sigma^i\boldsymbol{\partial}_+\cdot\boldsymbol{\partial}_-\chi+if_9 N^\dagger\sigma^i N\chi^\dagger\boldsymbol{\sigma}\cdot\boldsymbol{\partial}_+\partial_-^i\chi\\&+if_{10}N^\dagger\boldsymbol{\sigma}\cdot\boldsymbol{\partial}_+ N\chi^\dagger\boldsymbol{\sigma}\cdot\boldsymbol{\partial}_-\chi\Big\}+\mathcal{O}(1/m_N^6)\,.\end{aligned}\tag{86}$$

Relativistic invariance enforces the constraints

$$f_1+rf_2=f_5+rf_8=f_7+rf_9=f_6+rf_{10}=f_3=f_4=0\tag{87}$$

leaving four independent operators.

5.2.1 Lorentz versus Galilean invariance

We remark that the basis of operators in Eq. (79) under the constraints in (81) is Lorentz invariant. If in place of the transformations in (80) we instead enforced Galilean symmetry [21], defined by

$$N\to e^{im_N\boldsymbol{\eta}\cdot\boldsymbol{x}}N\,,\quad \chi\to e^{im_\chi\boldsymbol{\eta}\cdot\boldsymbol{x}}\chi\,,\quad \partial_t\to\partial_t-\boldsymbol{\eta}\cdot\boldsymbol{\partial}\,,\quad \boldsymbol{\partial}\to\boldsymbol{\partial}\,,\tag{88}$$

we would obtain constraints on dimension eight operators different from (81).[16] These constraints would imply that all Hermitian operators are constructed from the combinations of derivatives corresponding to

$$\boldsymbol{v}_{\rm rel} \equiv \frac{1}{2}\left[\frac{\boldsymbol{p}+\boldsymbol{p}'}{m_N} - \frac{\boldsymbol{k}+\boldsymbol{k}'}{m_\chi}\right], \quad \boldsymbol{q} \equiv \boldsymbol{p}' - \boldsymbol{p} = \boldsymbol{k} - \boldsymbol{k}', \tag{89}$$

where p and k (p' and k') are the incoming (outgoing) momenta of N and χ respectively. In particular, the violation of Lorentz symmetry obtained by using (88) in place of (80) would manifest itself as the absence of operators coupling to total momentum $\boldsymbol{P}$,

$$\boldsymbol{P} \equiv \boldsymbol{p} + \boldsymbol{k} = \boldsymbol{p}' + \boldsymbol{k}'. \tag{90}$$

Note that Lorentz symmetry links a leading order nucleon spin-dependent operator (d_1) to subleading nucleon spin-independent operators. The phenomenological impact of such terms remains to be investigated. Note that Lorentz symmetry cannot be obtained by enforcing additional constraints on operators present in the Galilean invariant theory.

6 Phenomenological illustrations

The forgoing analysis provides a framework to systematically evolve coefficients defined at the weak scale, to obtain the effective low-energy theory where nuclear matrix elements are evaluated. As illustration we focus attention on two cases: firstly the specification of contact interactions at or above the weak scale, and secondly, the specification of the complete basis of coefficients at the weak scale by the leading order of the heavy WIMP expansion.

6.1 Contact interactions

Consider the contact interactions between a Majorana fermion WIMP and SM fields given in Eq. (6). As a simple illustration, let us focus on the set of operators

$$\mathcal{L}_{\chi,SM} = \frac{1}{\Lambda^2}\bar{\chi}\chi\left[b_u\bar{u}u + b_d\bar{d}d + \frac{b_g}{\Lambda}(G^a_{\mu\nu})^2\right], \tag{91}$$

where coefficients $b_{u,d,g}$ may be constrained by collider production bounds [17] or engineered to produce a desired WIMP-nucleus scattering phenomenology [83]. An observable of interest for the latter is the ratio f_n/f_p of the effective spin-independent WIMP-neutron (f_n) and WIMP-proton (f_p) couplings.[17]

We show in Fig. 1 predictions for f_n/f_p from the model in Eq. (91), highlighting large effects from hadronic matrix element uncertainties and the choice of QCD renormalization scale. The left panel illustrates uncertainties from varying the SM quantities Σ_- and $R_{ud} = m_u/m_d$ given in (58) and (60).[18] The right panel illustrates the uncertainty from not specifying the renormalization scale at which the coefficients b_i are defined. Meaningful predictions for f_n/f_p require both a precise knowledge of hadronic inputs and a careful treatment of renormalization effects. Similar considerations apply to other applications that relate constraints on contact interactions at the electroweak scale to low energy observables such as direct detection cross sections or annihilation rates for low mass WIMPs.

[16] Galilean constraints would be given by the formal limit $d_1 = d_2 = 0$ in (81).

[17] In terms of the couplings in (79), f_p and f_n are proportional to $d_2^{(p)}$ and $d_2^{(n)}$, respectively.

[18] The point $-b_u/b_d = 1.08$ was highlighted in [83]. Hadronic uncertainties are severe at this point. The uncertainty from Σ_- may be reduced by employing the analysis in Ref. [76].

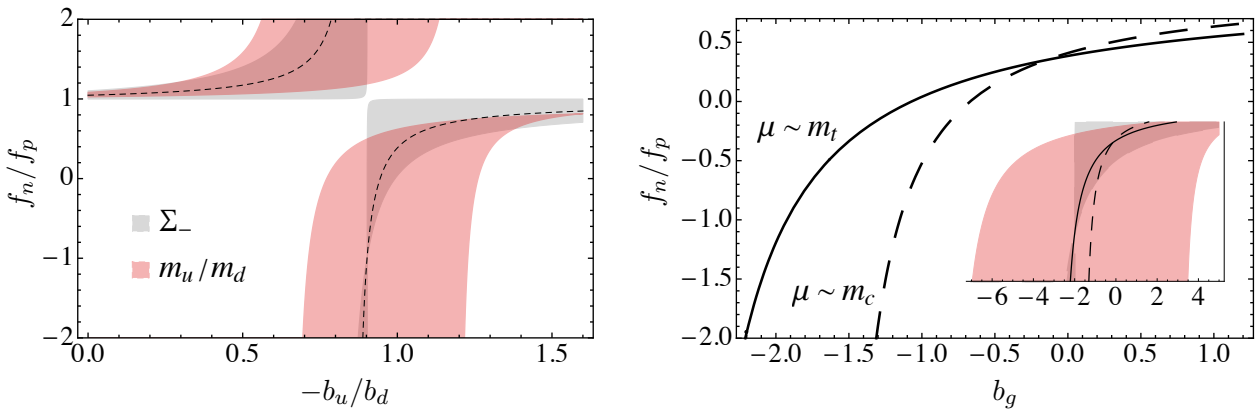

Figure 1: The ratio f_n/f_p of the effective WIMP-neutron (f_n) and WIMP-proton (f_p) couplings in terms of the parameters b_i in Eq. (91). For $b_g = 0$ (left panel), f_n/f_p is independent of Λ and depends on only the ratio b_u/b_d. The uncertainty bands are from variation of the matrix element Σ_- (gray) and the ratio $R_{ud} = m_u/m_d$ (red), with ranges given in (58) and (60). We illustrate the effect of non-zero b_g in the right panel, with $b_d = -b_u = 0.01$ and $\Lambda = 400\,\text{GeV}$. The solid (dashed) line is the prediction assuming that the coefficients b_i are defined at a high (low) scale $\mu \sim m_t$ ($\mu \sim m_c$). The inset shows the curves over the same vertical range, including uncertainty bands for the solid line from variation of Σ_- (gray) and R_{ud} (red). In both cases the variation from $\Sigma_{\pi N}$ is subdominant.

6.2 Heavy, electroweak-charged WIMPs

We consider the heavy WIMP limit ($M \gg m_W$) for the cases of a self-conjugate electroweak triplet of hypercharge zero ("wino-like"), and an electroweak doublet of hypercharge 1/2 ("higgsino-like"). For the latter, we assume mass perturbations that cause the mass eigenstates after EWSB to be self-conjugate combinations, thus forbidding a phenomenologically disfavored tree-level vector coupling between the lightest electrically neutral state and Z^0 (see Section 4 of Ref. [4] for details). The bare effective lagrangian at the weak-scale describing interactions of the lightest electrically neutral self-conjugate WIMP (of arbitrary spin) with low-energy SM degrees of freedom is given by

$$\mathcal{L}_{\chi_v,\,\text{SM}} = \bar{\chi}_v \chi_v \left\{ \sum_{q=u,d,s,c,b} \left[c_q^{(0)} O_q^{(0)} + c_q^{(2)} v_\mu v_\nu O_q^{(2)\mu\nu} \right] + c_g^{(0)} O_g^{(0)} + c_g^{(2)} v_\mu v_\nu O_g^{(2)\mu\nu} \right\} + \dots , \qquad (92)$$

where the scalar and C-even spin-two operators, $O_{q,g}^{(0)}$ and $O_{q,g}^{(2)}$, are given in Table 2, and the coefficients are defined to include the mass suppression $1/m_W^3$. The bare matching coefficients for both wino-like and higgsino-like cases were computed explicitly in Ref. [4] and are reproduced here for completeness:[19]

$$c_U^{(0)} = \frac{\pi\Gamma(1+\epsilon) g_2^4}{(4\pi)^{2-\epsilon}} \left\{ -\frac{m_W^{-3-2\epsilon}}{2x_h^2} \left[\mathcal{C}_W + \frac{\mathcal{C}_Z}{c_W^3} \right] + \frac{m_Z^{-3-2\epsilon} \mathcal{C}_Z}{8 c_W^4} \left[c_V^{(U)2} - c_A^{(U)2} \right] + \mathcal{O}(\epsilon) \right\},$$

$$c_D^{(0)} = \frac{\pi\Gamma(1+\epsilon) g_2^4}{(4\pi)^{2-\epsilon}} \left\{ -\frac{m_W^{-3-2\epsilon}}{2x_h^2} \left[\mathcal{C}_W + \frac{\mathcal{C}_Z}{c_W^3} \right] + \frac{m_Z^{-3-2\epsilon} \mathcal{C}_Z}{8 c_W^4} \left[c_V^{(D)2} - c_A^{(D)2} \right] \right.$$

[19] Spin-0 results were also obtained in [84].

$$
\left. - \delta_{Db}\, m_W^{-3-2\epsilon} \mathcal{C}_W \frac{x_t}{8(x_t+1)^3} + \mathcal{O}(\epsilon) \right\},
$$

$$
c_g^{(0)} = \frac{\pi[\Gamma(1+\epsilon)]^2 g_2^4 g^2}{(4\pi)^{4-2\epsilon}} \left\{ \frac{m_W^{-3-4\epsilon}}{2} \left[\frac{1}{3x_h^2} \left[\mathcal{C}_W + \frac{\mathcal{C}_Z}{c_W^3} \right] + \mathcal{C}_W \left[\frac{1}{3} + \frac{1}{6(x_t+1)^2} \right] \right] \right.
$$

$$
+ \frac{m_Z^{-3-4\epsilon} \mathcal{C}_Z}{64 c_W^4} \left[4\left[c_V^{(D)2} + c_A^{(D)2} \right] + \left[c_V^{(U)2} + c_A^{(U)2} \right] \left[\frac{8}{3} + \frac{32 y_t^6 (8y_t^2 - 7)}{(4y_t^2-1)^{7/2}} \arctan\left(\sqrt{4y_t^2 - 1} \right) \right. \right.
$$

$$
\left. - \pi y_t + \frac{4(48 y_t^6 - 2y_t^4 + 9y_t^2 - 1)}{3(4y_t^2-1)^3} \right] + \left[c_V^{(U)2} - c_A^{(U)2} \right] \left[3\pi y_t - \frac{4(144 y_t^6 - 70 y_t^4 + 9y_t^2 - 2)}{3(4y_t^2-1)^3} \right.
$$

$$
\left. \left. \left. - \frac{32 y_t^4 (24 y_t^4 - 21 y_t^2 + 5)}{(4y_t^2-1)^{7/2}} \arctan\left(\sqrt{4y_t^2 - 1} \right) \right] \right] + \mathcal{O}(\epsilon) \right\},
$$

$$
c_U^{(2)} = \frac{\pi \Gamma(1+\epsilon) g_2^4}{(4\pi)^{2-\epsilon}} \left\{ \left[m_W^{-3-2\epsilon} \mathcal{C}_W + \frac{m_Z^{-3-2\epsilon} \mathcal{C}_Z}{2 c_W^4} \left[c_V^{(U)2} + c_A^{(U)2} \right] \right] \left[\frac{1}{3} + \left(\frac{11}{9} - \frac{2}{3} \log 2 \right) \epsilon \right] + \mathcal{O}(\epsilon^2) \right\},
$$

$$
c_D^{(2)} = \frac{\pi \Gamma(1+\epsilon) g_2^4}{(4\pi)^{2-\epsilon}} \left\{ \left[m_W^{-3-2\epsilon} \mathcal{C}_W + \frac{m_Z^{-3-2\epsilon} \mathcal{C}_Z}{2 c_W^4} \left[c_V^{(D)2} + c_A^{(D)2} \right] \right] \left[\frac{1}{3} + \left(\frac{11}{9} - \frac{2}{3} \log 2 \right) \epsilon \right] \right.
$$

$$
+ \delta_{Db} \frac{m_W^{-3-2\epsilon} \mathcal{C}_W}{2} \left[\frac{(3x_t+2)}{3(x_t+1)^3} - \frac{2}{3} + \left(\frac{2x_t(7x_t^2-3)}{3(x_t^2-1)^3} \log x_t - \frac{2(3x_t+2)}{3(x_t+1)^3} \log 2 \right. \right.
$$

$$
\left. \left. - \frac{2(25x_t^2 - 2x_t - 11)}{9(x_t^2-1)^2(x_t+1)} - \frac{22}{9} + \frac{4}{3} \log 2 \right) \epsilon \right] + \mathcal{O}(\epsilon^2) \left. \right\},
$$

$$
c_g^{(2)} = \frac{\pi[\Gamma(1+\epsilon)]^2 g_2^4 g^2}{(4\pi)^{4-2\epsilon}} \left\{ \frac{m_W^{-3-4\epsilon} \mathcal{C}_W}{2} \left[- \frac{16}{9\epsilon} - \frac{284}{27} + \frac{32}{9} \log 2 - \frac{2(3x_t+2)}{9(x_t+1)^3} \frac{1}{\epsilon} \right. \right.
$$

$$
+ \frac{8(6x_t^8 - 18x_t^6 + 21x_t^4 - 3x_t^2 - 2)}{9(x_t^2-1)^3} \log(x_t+1) + \frac{4(3x_t^4 - 21x_t^3 + 3x_t^2 + 9x_t - 2)}{9(x_t^2-1)^3} \log 2
$$

$$
- \frac{4(12x_t^8 - 36x_t^6 + 39x_t^4 + 14x_t^3 - 9x_t^2 - 6x_t - 2)}{9(x_t^2-1)^3} \log x_t
$$

$$
\left. - \frac{144x_t^6 + 72x_t^5 - 312x_t^4 - 105x_t^3 - 40x_t^2 + 47x_t + 98}{27(x_t^2-1)^2(x_t+1)} \right]
$$

$$
+ \frac{m_Z^{-3-4\epsilon} \mathcal{C}_Z}{64 c_W^4} \left[\left[8\left[c_V^{(U)2} + c_A^{(U)2} \right] + 12\left[c_V^{(D)2} + c_A^{(D)2} \right] \right] \left[- \frac{16}{9\epsilon} - \frac{284}{27} + \frac{32}{9} \log 2 \right] \right.
$$

$$
+ \left[c_V^{(U)2} + c_A^{(U)2} \right] \left[\frac{128(24 y_t^8 - 21 y_t^6 - 4y_t^4 + 5y_t^2 - 1)}{9(4y_t^2-1)^{7/2}} \arctan\left(\sqrt{4y_t^2 - 1} \right) - \frac{4\pi y_t}{3} \right.
$$

$$
\left. \left. + \frac{16(48 y_t^6 + 62 y_t^4 - 47 y_t^2 + 9)}{9(4y_t^2-1)^3} \right] + \left[c_V^{(U)2} - c_A^{(U)2} \right] \left[\frac{16 y_t^2 (624 y_t^4 - 538 y_t^2 + 103)}{9(4y_t^2-1)^3} - \frac{52\pi y_t}{3} \right. \right.
$$

$$+\frac{128y_t^2(104y_t^6-91y_t^4+35y_t^2-5)}{3(4y_t^2-1)^{7/2}}\arctan\left(\sqrt{4y_t^2-1}\right)\Bigg]\Bigg]+\mathcal{O}(\epsilon)\Bigg\}, \tag{93}$$

where $x_i = m_i/m_W$, $y_i = m_i/m_Z$ and

$$c_V^{(U)} = 1-\frac{8}{3}s_W^2\,, \quad c_V^{(D)} = -1+\frac{4}{3}s_W^2\,, \quad c_A^{(U)} = -1\,, \quad c_A^{(D)} = 1\,. \tag{94}$$

We denote generic up- and down-type quarks by U and D, respectively, and the Kronecker delta, δ_{Db}, is equal to unity for $D = b$, and vanishes for $D = d, s$. We have used CKM unitarity, $\sum_D |V_{UD}|^2 = 1$, to simplify the results; in practice it is sufficient to set $V_{tb} = 1$ for the numerical analysis. Beyond the specification of the WIMP electroweak quantum numbers J and Y through the constants

$$\mathcal{C}_W = [J(J+1)-Y^2]\,, \quad \mathcal{C}_Z = Y^2, \tag{95}$$

the matching coefficients are completely given by SM parameters in the heavy WIMP limit. The wino-like and higgsino-like results are obtained by setting $\mathcal{C}_W = 2\,, \mathcal{C}_Z = 0$ and $\mathcal{C}_W = 1/2\,, \mathcal{C}_Z = 1/4$, respectively.

Let us now consider the evolution down to low energies for these weak scale coefficients, and the subsequent evaluation of hadronic matrix elements to obtain the benchmark low-velocity single-nucleon scattering cross section.

6.2.1 Coefficient renormalization

Let us employ $Z^{(0)}$ and $Z^{(2)}$ through $\mathcal{O}(\alpha_s)$ given in Table 3 to derive the relation between bare and renormalized coefficients at first non-vanishing order. From the definition in (15), the renormalized coefficients for the scalar operators are

$$\begin{aligned} c_q^{(0)}(\mu) &= \sum_{q'} Z_{q'q}^{(0)}(\mu) c_{q'}^{(0)\text{bare}} + Z_{gq}^{(0)}(\mu) c_g^{(0)\text{bare}} = c_q^{(0)\text{bare}} + \mathcal{O}(\alpha_s^2)\,, \\ c_g^{(0)}(\mu) &= \sum_{q'} Z_{q'g}^{(0)}(\mu) c_{q'}^{(0)\text{bare}} + Z_{gg}^{(0)}(\mu) c_g^{(0)\text{bare}} = c_g^{(0)\text{bare}} + \mathcal{O}(\alpha_s^2)\,, \end{aligned} \tag{96}$$

while for the C-even spin-two operators, we find

$$\begin{aligned} c_q^{(2)}(\mu) &= \sum_{q'} Z_{q'q}^{(2)}(\mu) c_{q'}^{(2)\text{bare}} + Z_{gq}^{(2)}(\mu) c_g^{(2)\text{bare}} = c_q^{(2)\text{bare}} + \mathcal{O}(\alpha_s)\,, \\ c_g^{(2)}(\mu) &= \sum_{q'} Z_{q'g}^{(2)}(\mu) c_{q'}^{(2)\text{bare}} + Z_{gg}^{(2)}(\mu) c_g^{(2)\text{bare}} = \sum_q \frac{1}{\epsilon}\frac{\alpha_s}{6\pi} c_q^{(2)\text{bare}} + c_g^{(2)\text{bare}} + \mathcal{O}(\alpha_s^2)\,. \end{aligned} \tag{97}$$

In particular, a nontrivial subtraction requiring the $\mathcal{O}(\epsilon)$ part of the coefficients $c_q^{(2)\text{bare}}$ is necessary to obtain the renormalized coefficient $c_g^{(2)}(\mu)$. Employing (96) and (97), we find the renormalized coefficients

$$\begin{aligned} c_U^{(0)}(\mu) &= \frac{\pi\alpha_2^2}{m_W^3}\Bigg\{-\frac{1}{2x_h^2}\left[\mathcal{C}_W+\frac{\mathcal{C}_Z}{c_W^3}\right]+\frac{\mathcal{C}_Z}{8c_W}\left[c_V^{(U)2}-c_A^{(U)2}\right]\Bigg\}, \\ c_D^{(0)}(\mu) &= \frac{\pi\alpha_2^2}{m_W^3}\Bigg\{-\frac{1}{2x_h^2}\left[\mathcal{C}_W+\frac{\mathcal{C}_Z}{c_W^3}\right]+\frac{\mathcal{C}_Z}{8c_W}\left[c_V^{(D)2}-c_A^{(D)2}\right]-\delta_{Db}\,\mathcal{C}_W\frac{x_t}{8(x_t+1)^3}\Bigg\}, \end{aligned}$$

$$
\begin{aligned}
c_g^{(0)}(\mu) = \frac{\pi\alpha_2^2}{m_W^3}\frac{\alpha_s(\mu)}{4\pi}\Bigg\{ & \frac{1}{2}\Bigg[\frac{1}{3x_h^2}\left[\mathcal{C}_W + \frac{\mathcal{C}_Z}{c_W^3}\right] + \mathcal{C}_W\left[\frac{1}{3} + \frac{1}{6(x_t+1)^2}\right]\Bigg] \\
& + \frac{\mathcal{C}_Z}{64c_W}\Bigg[4\left[c_V^{(D)2} + c_A^{(D)2}\right] + \left[c_V^{(U)2} + c_A^{(U)2}\right]\Bigg[\frac{8}{3} + \frac{32y_t^6(8y_t^2-7)}{(4y_t^2-1)^{7/2}}\arctan\left(\sqrt{4y_t^2-1}\right) \\
& - \pi y_t + \frac{4(48y_t^6 - 2y_t^4 + 9y_t^2 - 1)}{3(4y_t^2-1)^3}\Bigg] + \left[c_V^{(U)2} - c_A^{(U)2}\right]\Bigg[3\pi y_t - \frac{4(144y_t^6 - 70y_t^4 + 9y_t^2 - 2)}{3(4y_t^2-1)^3} \\
& - \frac{32y_t^4(24y_t^4 - 21y_t^2 + 5)}{(4y_t^2-1)^{7/2}}\arctan\left(\sqrt{4y_t^2-1}\right)\Bigg]\Bigg]\Bigg\}, \\
c_U^{(2)}(\mu) = \frac{\pi\alpha_2^2}{m_W^3}\Bigg\{ & \frac{\mathcal{C}_W}{3} + \frac{\mathcal{C}_Z}{6c_W}\left[c_V^{(U)2} + c_A^{(U)2}\right]\Bigg\}, \\
c_D^{(2)}(\mu) = \frac{\pi\alpha_2^2}{m_W^3}\Bigg\{ & \frac{\mathcal{C}_W}{3} + \frac{\mathcal{C}_Z}{6c_W}\left[c_V^{(D)2} + c_A^{(D)2}\right] + \delta_{Db}\,\frac{\mathcal{C}_W}{2}\left[\frac{(3x_t+2)}{3(x_t+1)^3} - \frac{2}{3}\right]\Bigg\}, \\
c_g^{(2)}(\mu) = \frac{\pi\alpha_2^2}{m_W^3}\frac{\alpha_s(\mu)}{4\pi}\Bigg\{ & \mathcal{C}_W\Bigg[-\frac{2(8x_t^3 + 24x_t^2 + 27x_t + 10)}{9(x_t+1)^3}\log\frac{\mu}{m_W} - \frac{4x_t(7x_t^2-3)}{9(x_t^2-1)^3}\log 2 \\
& - \frac{2(12x_t^5 - 36x_t^4 + 36x_t^3 - 12x_t^2 + 3x_t - 2)}{9(x_t-1)^3}\log x_t \\
& + \frac{4(6x_t^8 - 18x_t^6 + 21x_t^4 - 3x_t^2 - 2)}{9(x_t^2-1)^3}\log(x_t+1) \\
& - \frac{48x_t^6 + 60x_t^5 - 68x_t^4 - 107x_t^3 - 52x_t^2 + 49x_t + 54}{18(x_t^2-1)^2(x_t+1)}\Bigg] \\
& + \frac{\mathcal{C}_Z}{c_W}\Bigg[\left[2\left[c_V^{(U)2} + c_A^{(U)2}\right] + 3\left[c_V^{(D)2} + c_A^{(D)2}\right]\right]\left[-\frac{1}{4} - \frac{2}{9}\log\frac{\mu}{m_Z}\right] + \left[c_V^{(U)2} + c_A^{(U)2}\right]\Bigg[-\frac{\pi y_t}{48} \\
& + \frac{2(24y_t^8 - 21y_t^6 - 4y_t^4 + 5y_t^2 - 1)}{9(4y_t^2-1)^{7/2}}\arctan\left(\sqrt{4y_t^2-1}\right) + \frac{48y_t^6 + 62y_t^4 - 47y_t^2 + 9}{36(4y_t^2-1)^3}\Bigg] \\
& + \left[c_V^{(U)2} - c_A^{(U)2}\right]\Bigg[-\frac{13\pi y_t}{48} + \frac{2y_t^2(104y_t^6 - 91y_t^4 + 35y_t^2 - 5)}{3(4y_t^2-1)^{7/2}}\arctan\left(\sqrt{4y_t^2-1}\right) \\
& + \frac{y_t^2(624y_t^4 - 538y_t^2 + 103)}{36(4y_t^2-1)^3}\Bigg]\Bigg]\Bigg\}. \qquad (98)
\end{aligned}
$$

We proceed to study the evolution of these coefficients down to low-energies.

6.2.2 Coefficient evolution

Let us illustrate the evolution of scalar and C-even spin-two coefficients from a high scale down to a low scale, employing the solutions for RG running and threshold matching, R and M, given in

	$c^{(0)}_{u,d,s}$	$c^{(0)}_c$	$c^{(0)}_b$	$c^{(0)}_g$	$c^{(2)}_{u,d,s}$	$c^{(2)}_c$	$c^{(2)}_b$	$c^{(2)}_g$
μ_t	-0.407	-0.407	-0.424	0.004	0.667	0.667	0.091	-0.050
μ_b	-0.418	-0.418	-0.436	0.009	0.498	0.498	0.073	0.080
μ_b	-0.418	-0.418	-	0.012	0.498	0.498	-	0.080
μ_c	-0.443	-0.443	-	0.022	0.418	0.418	-	0.140
μ_c	-0.443	-	-	0.028	0.418	-	-	0.140
μ_0	-0.454	-	-	0.032	0.405	-	-	0.147

Table 14: Evolution of scalar (left panel) and C-even spin-two (right panel) coefficients for the pure triplet (with overall factors $\pi\alpha_2^2/m_W^3$ extracted) from a high scale, μ_t, down to a low scale, μ_0. The number of active quark flavors changes at heavy quark thresholds μ_b and μ_c for the bottom and charm, respectively. Isospin symmetry and $|V_{tb}| \approx 1$ lead to identical results for u, d, s.

Tables 5 and 6. For definiteness, we consider the high scale coefficients given by the renormalized coefficients in (98) for an electroweak triplet (i.e., a pure wino). Results for an electroweak doublet (i.e., a pure Higgsino) are qualitatively similar. For illustration, we choose the default scale values $\mu_t = (m_t + m_W)/2 \approx 126$ GeV, $\mu_b = 4.75$ GeV, $\mu_c = 1.4$ GeV and $\mu_0 = 1.2$ GeV.

The results for scalar coefficients presented in the left panel of Table 14 employ $R^{(0)}$ and $M^{(0)}$ at NLO. The high-scale gluon coefficient is small, having a factor of $\alpha_s(\mu_t)$, but increases at lower scales due to running and heavy quark threshold effects. A large nucleon matrix element for the gluon makes it a dominant contribution to the scattering cross section.

In the present example, mixing between the scalar quark and gluon operators shift the quark coefficients by $\mathcal{O}(5-10\%)$. For applications with only a gluon coefficient $c_g^{(0)}(\mu_t)$ at the high scale, the mixing would induce nonzero quark coefficients at the low scale, e.g., $c_q^{(0)}(\mu_b) = -2.8 c_g^{(0)}(\mu_t)$, and could be phenomenologically relevant.

The results for C-even spin-two coefficients presented in the right panel of Table 14 employ $R^{(2)}$ and $M^{(2)}$ at LO. The high-scale gluon coefficient is $\mathcal{O}(10\%)$ of the u, d, s, c quark coefficients, and contains a large uncertainty of $\pm\mathcal{O}(40\%)$ from scale variation of μ_t. Hence, the C-even spin-two gluon coefficient is required for a robust estimate of perturbative uncertainties. In the next section, we will see that due to destructive interference between the scalar and C-even spin-two amplitudes, the gluon coefficient has a sizable impact on scattering cross sections of heavy WIMPs.

6.2.3 Amplitudes and cross section predictions

Let us evaluate the scalar and C-even spin-two amplitudes in the 3-flavor theory at a low scale μ_0 to determine the scattering cross section for heavy electroweak charged dark matter.[20] From the coefficients of the previous section and the matrix elements discussed in Sec. 4, the amplitudes are given by

$$\mathcal{M}_N^{(S)} = \sum_{i=u,d,s,g} c_i^{(S)}(\mu_0) \langle N | O_i^{(S)}(\mu_0) | N \rangle \,. \tag{99}$$

[20] As previously discussed, the C-even spin-two matrix elements are parametrized in terms of PDF moments and may thus be evaluated directly at the high scale.

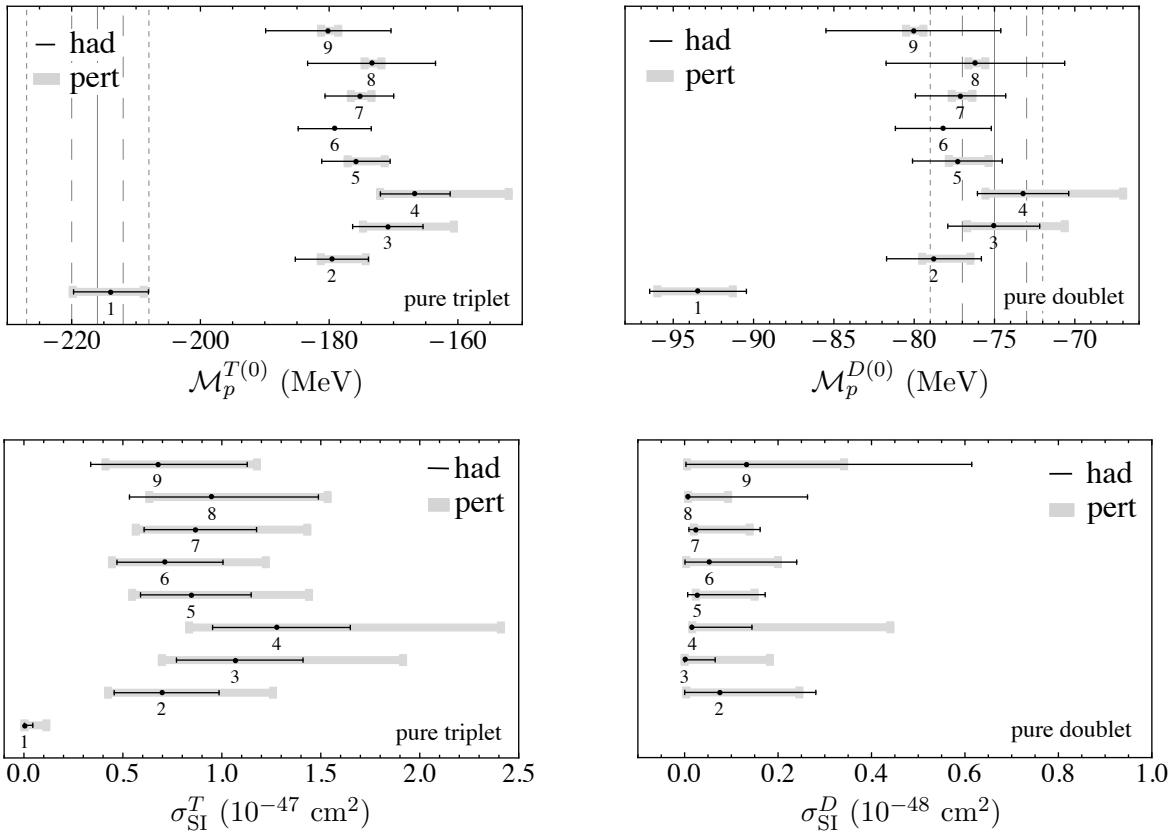

Figure 2: Scalar amplitudes (upper panels) and spin-independent cross sections (lower panels) for the pure triplet (left panel) and pure doublet (right panel) cases. The perturbative (hadronic) uncertainties are denoted by thick gray (thin black) lines, and we have extracted the factor $\pi\alpha_s^2/m_W^3$ from the amplitudes. Vertical lines denote the magnitude of the C-even spin-two amplitude (solid) and its perturbative (short dash) and hadronic (long dash) uncertainties as given in Eq. (100). We describe each evaluation (labelled 1 through 9) in the text. For the pure doublet, the cross section corresponding to amplitude 1 is not shown.

For the cases of pure triplet and pure doublet scattering on a proton target, we find the C-even spin-two ($S = 2$) amplitudes

$$\mathcal{M}_p^{T(2)} = \frac{\pi\alpha_2^2}{m_W^3}\left[216\left({}^{+11}_{-8}\right)\left({}^{+4}_{-4}\right)\text{ MeV}\right], \quad \mathcal{M}_p^{D(2)} = \frac{\pi\alpha_2^2}{m_W^3}\left[75\left({}^{+4}_{-3}\right)\left({}^{+2}_{-2}\right)\text{ MeV}\right], \tag{100}$$

where the superscripts T and D denote triplet and doublet, respectively. The first uncertainty is from scale variation, while the second is from PDF inputs. We neglect the uncertainties from variation of μ_b, μ_c and μ_0 which are of $\mathcal{O}(1\%)$. The amplitudes for scattering on a neutron are numerically similar.

For the scalar amplitude ($S = 0$) we present several evaluations in the upper panels of Fig. 2 to illustrate the impact of perturbative QCD corrections. The amplitudes numbered 1 through 4 employ NLO solutions for the running from μ_t to μ_c and for the matching at the bottom and charm thresholds. Below the charm threshold, amplitudes 1, 2, 3 and 4 respectively employ LO, NLO, NNLO and NNNLO in the running to the low scale μ_0 and in the scalar gluon matrix element determined from the sum rule.[21] For amplitudes 1, 2, 3 and 4, the scale μ_c dominates the perturbative uncertainty.

The increased uncertainty in amplitudes 3 and 4 reflects $\alpha_s(\mu_c)$ corrections to the charm threshold matching and to the running from μ_b to μ_c beyond the included NLO corrections; i.e., reduction of the μ_c scale dependence requires a cancellation between $\alpha_s(\mu_c)$ corrections above, at and below the charm scale. The new corrections to threshold matching obtained in Sec. 3.5 provide the missing ingredients required for such a higher order analysis. Including corrections through NNNLO to the running from μ_b to μ_c and to the charm threshold matching (employing (37), (38) and Ref. [51] for M_{gQ} and M_{qQ}), we obtain amplitude 5 with reduced perturbative uncertainty.

The framework described in terms of the solutions R and M is equivalent to a perturbative determination of the scalar amplitude. The μ_0 dependence cancels between the gluon matrix element and the running below the charm threshold, yielding a result depending on the scales μ_t, μ_b and μ_c only. Working through NLO, we obtain the amplitude

$$\begin{aligned}
\frac{\mathcal{M}_N^{(0)}}{m_N} &= \sum_{q=u,d,s} f_{q,N}^{(0)} c_q^{(0)}(\mu_t) + \frac{2}{27}(1-\lambda)c_c^{(0)}(\mu_t)\left\{1 + \frac{\alpha_s^{(4)}(\mu_c)}{4\pi}\left[\frac{107}{9} - \frac{8}{1-\lambda}\right]\right\} \\
&\quad + \frac{2}{27}(1-\lambda)c_b^{(0)}(\mu_t)\left\{1 + \frac{\alpha_s^{(4)}(\mu_c)}{4\pi}\left[-\frac{214}{225} + \frac{16}{25(1-\lambda)}\right] + \frac{\alpha_s^{(5)}(\mu_b)}{4\pi}\left[\frac{321}{25} - \frac{216}{25(1-\lambda)}\right]\right\} \\
&\quad - \frac{8\pi}{9\alpha_s^{(6)}(\mu_t)} f_N^{(0)} c_g(\mu_t)\left\{1 + \frac{\alpha_s^{(4)}(\mu_c)}{4\pi}\left[-\frac{214}{225} + \frac{16}{25(1-\lambda)}\right] + \frac{\alpha_s^{(5)}(\mu_b)}{4\pi}\left[-\frac{642}{575} + \frac{432}{575(1-\lambda)}\right]\right. \\
&\quad \left. + \frac{\alpha_s^{(6)}(\mu_t)}{4\pi}\left[\frac{68}{23} - \frac{216}{23(1-\lambda)} + \frac{4}{3}\log\frac{\mu_t}{m_t}\right]\right\} + \mathcal{O}(\alpha_s^2, 1/m_c, 1/m_b, 1/m_N)\,,
\end{aligned} \tag{101}$$

where $\lambda = \sum_{q=u,d,s} f_{q,N}^{(0)}$, and the leading-order α_s result is well-known from Ref. [85]. Since the quark matrix elements are scale independent and, neglecting power corrections, are not corrected at heavy quark thresholds, the result in Eq. (101) is the same whether obtained in a 4- or 5-flavor

[21] The amplitudes 1, 2, 3, and 4 shown here correspond to the cross sections labelled LO, NLO, NNLO and NNNLO in Figure 1 of Ref. [16].

theory employing the NLO solution given in (39) for the charm and bottom matrix elements. Given the ingredients in Sec. 3.5, it is straightforward to extend this result to NNNLO. For illustration, we include in Fig. 2 the amplitudes corresponding to the LO and NLO result in Eq. (101), labelled 6 and 7, respectively. The LO result has no scale variation, while the NLO result gives an estimate of perturbative corrections that is consistent with amplitudes 2 and 5, albeit smaller.[22]

The amplitudes 8 and 9 in Fig. 2 are evaluated in the 4-flavor theory, employing the charm matrix elements given in (62). The large hadronic uncertainty reflects those of the lattice measurements, while the scale uncertainty is small, having avoided a perturbative treatment of the scale μ_c.

The cross section for scattering on a nucleon target is obtained from the amplitudes as

$$\sigma_{\rm SI} = \frac{m_N^2}{\pi} |\mathcal{M}_N^{(0)} + \mathcal{M}_N^{(2)}|^2 \,. \tag{102}$$

In the case of heavy electroweak-charged WIMPs, opposite signs of the scalar and C-even spin-two amplitudes lead to destructive interference. There is a large cancellation for scalar amplitudes near the vertical lines denoting the magnitude of the C-even spin-two amplitude in the upper panels of Fig. 2. Cross section predictions are shown in the lower panels with labels corresponding to the scalar amplitude employed.

For the triplet, the cross section prediction given in Ref. [16] corresponds to amplitude 4 in Fig. 2, and gives a conservative estimate of scale uncertainty. An improved estimate with reduced scale uncertainty is given by the cross section corresponding to amplitude 5,

$$\sigma_{\rm SI}^T = 8^{+6+3}_{-3-3} \times 10^{-48}\ {\rm cm}^2 \,, \tag{103}$$

where the first (second) uncertainty is from scale variation (hadronic inputs). The remaining scale uncertainty is dominated by μ_t variation in the C-even spin-two amplitude, and its reduction requires higher-order matching at the weak-scale.

For the doublet case, the improved estimates lead to the same conclusion in Ref. [16],

$$\sigma_{\rm SI}^D \lesssim 10^{-48}\ {\rm cm}^2 \quad (95\%\ {\rm C.L.}) \,. \tag{104}$$

In the case of strong destructive interference, the cross section prediction and its fractional uncertainty become highly sensitive to perturbative corrections and changes in parameter inputs.

7 Summary and discussion

The analysis of WIMP dark matter scattering on an atomic nucleus is a challenging field theory problem involving multiple energy scales, ranging from mass scales of SM extensions ($\gtrsim$ TeV), to the electroweak scale ($\sim 100\,{\rm GeV}$), heavy quark thresholds ($\sim 5\,{\rm GeV}$), QCD and pion mass scales ($\sim 100\,{\rm MeV}$), nuclear excitation scales ($\sim$ MeV), and finally recoil energies in direct detection experiments ($\sim$ keV). A sequence of effective theories capitalizes on these scale separations, permitting a systematic expansion in small ratios such as $m_W/M_{\rm DM}$, m_b/m_W and $\Lambda_{\rm QCD}/m_c$. A corresponding sequence of matching computations and renormalization group evolution provides the connection between the parameters of high scale physics models and low energy observables. The preceding paper [4] of this series treated the problem of weak scale matching, which may proceed from a specified UV completion, or employ the heavy WIMP expansion to compute matching coefficients independent

[22] For amplitudes 2 and 5, we employ R and M matrices expanded order by order in α_s, and the residual scale uncertainty can be traced to spurious terms appearing in the product of these matrices.

of the detailed UV completion. The remaining steps in the sequence are independent of the origin of the weak scale matching coefficients, and in this paper we have treated the problem of relating the resulting theory renormalized at the weak scale to an effective theory renormalized at low scales ($\lesssim m_c$) where hadronic matrix elements are evaluated. We discussed some aspects of the further evaluation of nuclear matrix elements, and presented either the $n_f = 3$ flavor QCD theory, or the single nucleon theory discussed in Section 5, as a natural handoff point to detailed nuclear modeling.

Section 2 presented the basis of lagrangian interactions between scalar or fermion WIMPs and SM fields; for fermionic WIMPs, we considered photon interactions through dimension five, and quark or gluon interactions through dimension seven. These capture the leading interactions for either complex (Dirac) or self-conjugate (Majorana) WIMPs. A sample matching calculation onto this basis from a gauge-singlet WIMP UV completion was performed in 2.4; the case of electroweak charged dark matter was discussed in [4]. Seemingly dramatic effects can emerge when passing from high to low scales, generically involving processes that are naively absent but not forbidden by symmetry. Examples include the chiral rotation to mass eigenstates that induces an operator mediating spin-independent scattering, as considered in Section 2.4. Similarly, dipole interactions of WIMPs with the electromagnetic field ($c_{\chi 1}$ and $c_{\chi 2}$) can be induced by heavy quark loops from a theory which at some renormalization scale contains only contact interactions with quarks [86]. These examples highlight the importance of working in a low energy basis that is closed under renormalization, and that contains all operators not forbidden by symmetry. For self-conjugate WIMPs of mass $M \gtrsim m_W$, the $n_f + 1$ spin zero operators involving $O^{(0)}_{q,g}$ and $n_f + 1$ spin two operators involving $O^{(2)}_{q,g}$ in (92) determine spin independent interactions with nuclei. Remaining agnostic regarding UV completion, one could investigate direct detection constraints on these 12 coefficients ($n_f = 5$). Large redundancies in the parameters would appear since the effects of heavy quarks are degenerate with those of light quarks and gluons; passing to $n_f = 3$ leaves 8 coefficients that could be constrained in principle by a suite of direct detection observables. The spin zero operators $m_q \bar{q} q$ and $(G^a_{\mu\nu})^2$ have received most attention, but equally large contributions are obtained in many cases from spin two operators [16].

Section 3 considered the seven classes of QCD operators appearing in the basis for WIMP interactions with quarks and gluons. Each class is separately closed under QCD renormalization. Leading operator renormalization factors, anomalous dimensions, and threshold matching corrections were presented. Special attention was paid to the dimension four scalar operators, since this sector drives the final cross section uncertainty in many WIMP models. In particular, poor convergence of perturbation theory at the charm mass scale implies sensitivity of scattering observables to high orders in the α_s expansion. We performed a new analysis using sum rule constraints to derive the heavy quark threshold matching corrections for light quark and gluon interactions induced in the presence of a high scale gluon operator. To our knowledge, the expressions (38) are new. The solutions to RG evolution were obtained; combined with threshold matching corrections, these results provide the mapping of weak scale coefficients onto the low-energy theory containing the WIMP and $n_f = 3$ flavor QCD.

While a complete analysis of general nuclear matrix elements is beyond the scope of this work, in order to compute benchmark single nucleon cross sections, and make contact with nuclear models, Section 4 considers the nucleon matrix elements for each of the seven classes of relevant QCD operators. Again, special attention is paid to the scalar operator matrix elements. We provide an updated value for the perturbative prediction of the charm scalar matrix element in terms of $n_f = 3$ flavor QCD quark matrix elements. We surveyed current knowledge concerning the remaining nucleon matrix elements, providing a guide to the level of uncertainty in each case. Constraints on these matrix

elements arise from a wide range of techniques and approximations: elastic and inelastic electron and neutrino scattering; $SU(3)$ baryon spectroscopy and chiral perturbation theory; lattice QCD; and sum rule and anomaly constraints to relate gluon and quark matrix elements.

The significance of the remaining uncertainties depends on the WIMP model under investigation. Several matrix elements are also of relevance to nucleon electric dipole moment searches [87, 3] and remain a target for further improvement from lattice studies, or potentially (as concerns $F_A^{(p,0)}(0)$ in (49)) neutrino scattering [88, 89]. Let us single out several hadronic quantities that can be traced directly to significant (sometimes dramatic) uncertainties in WIMP models. The strange scalar matrix element is a well-known source of uncertainty in spin independent WIMP-nucleon scattering [90], as illustrated in Fig. 2. The quark mass ratio m_u/m_d and isovector scalar matrix element Σ_- in (58) drive an $O(1)$ uncertainty in connecting f_n/f_p to underlying quark-gluon operators in some well-studied scenarios (cf. Fig. 1). A charm scalar matrix significant different from the OPE (in $1/m_c$) prediction would significantly alter predictions for spin-independent scattering (cf. Fig. 3 of [16]). Clearly there is further room for significant, albeit model-dependent, impact from lattice QCD on dark matter direct detection.

For scenarios including light force mediators in the dark sector, we considered the heavy particle effective lagrangian for nucleons and WIMPs in Section 5. As discussed in Section 5.2.1, our basis differs (apart from notation) from a basis constrained by Galilean invariance [21] by the inclusion of operators forbidden by Galilean but not Lorentz invariance, and corresponding coefficient relations.

As phenomenological illustrations we considered two examples. The first involved relating contact interactions specified at the weak scale to the low-energy effective theory at hadronic scales. The chosen example exhibited a strong and previously unappreciated sensitivity of the ratio f_n/f_p (spin-independent WIMP nucleon couplings) to both hadronic matrix element uncertainties and QCD scale choice. The formalism presented here may be used to systematically relate more general classes of weak-scale contact interactions [91, 17] (and other) models to low energy observables of direct detection, or annihilation of low-mass WIMPs. The second phenomenological example provided details of the first complete calculation of the leading spin-independent WIMP-nucleon cross section in SM extensions consisting of one or two heavy ($M \gg m_W$) electroweak $SU(2)_W \times U(1)_Y$ multiplets. Inclusion of higher orders in perturbation theory for charm threshold corrections improves upon but does not significantly alter the conclusions previously reported in [15, 16]. While further analysis of power corrections and nuclear modeling is warranted, it is likely that such WIMP candidates will remain an elusive target for next generation direct detection searches [92, 93].

QCD corrections have an important impact on many WIMP models, and must be systematically incorporated in order to meaningfully compare theory and observation. A number of extensions can be readily considered, e.g., including new gauge interactions beyond the SM, higher spin DM, and inelastic scattering.

Acknowledgments

We thank Andreas Kronfeld for comments on the manuscript. This work was supported by the United States Department of Energy under Grant No. DE-FG02-13ER41958. MS acknowledges support from a Bloomenthal Fellowship at the University of Chicago, and from the Office of Science, Office of High Energy Physics, of the U.S. Department of Energy under contract DE-AC02-05CH11231.

A Renormalization constants

A.1 Finite corrections to the axial-vector and pseudoscalar renormalization constants

The renormalization constants given in Table 3 for the axial-vector currents and pseudoscalar operators include a finite correction in addition to the $\overline{\rm MS}$ scheme [39],

$$Z_A^{\rm singlet} = \left(Z_5^{\rm s}\right)^{-1}\left(Z_{\overline{\rm MS}}^{\rm s}\right)^{-1}, \quad Z_A^{\rm non-singlet} = \left(Z_5^{\rm ns}\right)^{-1}\left(Z_{\overline{\rm MS}}^{\rm ns}\right)^{-1}, \quad Z_{5qq}^{(0)} = Z_m\left(Z_5^{\rm P}\right)^{-1}\left(Z_{\overline{\rm MS}}^{\rm P}\right)^{-1}, \tag{105}$$

where

$$\begin{aligned}
Z_{\overline{\rm MS}}^{\rm ns} &= 1 + \left(\frac{\alpha_s}{4\pi}\right)^2 \frac{1}{\epsilon}\left(\frac{88}{3} - \frac{16}{9}n_f\right) + \mathcal{O}(\alpha_s^3)\,,\\
Z_5^{\rm ns} &= 1 + \frac{\alpha_s}{4\pi}\left(-\frac{16}{3}\right) + \mathcal{O}(\alpha_s^2)\,,\\
Z_{\overline{\rm MS}}^{\rm s} &= 1 + \left(\frac{\alpha_s}{4\pi}\right)^2 \frac{1}{\epsilon}\left(\frac{88}{3} + \frac{20}{9}n_f\right) + \mathcal{O}(\alpha_s^3)\,,\\
Z_5^{\rm s} &= 1 + \frac{\alpha_s}{4\pi}\left(-\frac{16}{3}\right) + \mathcal{O}(\alpha_s^2)\,,\\
Z_{\overline{\rm MS}}^{p} &= 1 + \frac{\alpha_s}{4\pi}\left(\frac{-4}{\epsilon}\right) + \left(\frac{\alpha_s}{4\pi}\right)^2\left[\left(30 - \frac{4}{3}n_f\right)\frac{1}{\epsilon^2} + \left(25 - \frac{22}{9}n_f\right)\frac{1}{\epsilon}\right] + \mathcal{O}(\alpha_s^3)\,,\\
Z_5^{p} &= 1 + \frac{\alpha_s}{4\pi}\left(-\frac{32}{3}\right) + \mathcal{O}(\alpha_s^2)\,.
\end{aligned} \tag{106}$$

The mass renormalization constant Z_m, also appearing in the renormalization constant Z_T of the antisymmetric tensor current T_q, is given by

$$Z_m = 1 + \frac{\alpha_s}{4\pi}\frac{1}{\epsilon}(-4) + \left(\frac{\alpha_s}{4\pi}\right)^2\left[\frac{1}{\epsilon^2}\left(30 - \frac{4}{3}n_f\right) + \frac{1}{\epsilon}\left(-\frac{101}{3} + \frac{10}{9}n_f\right)\right] + \mathcal{O}(\alpha_s^3)\,. \tag{107}$$

Terms contributing to one-loop matching and two-loop anomalous dimension are retained in the renormalization constants in (106) and in $Z_{5gq}^{(0)}$ and $Z_{5gg}^{(0)}$ given in Table 3.[23]

A.2 QCD beta function and quark anomalous dimension

The renormalization constant for the scalar operators is given in terms of the QCD beta function β and the quark mass anomalous dimension γ_m. We define these as

$$\begin{aligned}
\frac{\beta}{g} &= \frac{d\log g}{d\log\mu} = -\beta_0\left(\frac{\alpha_s}{4\pi}\right) - \beta_1\left(\frac{\alpha_s}{4\pi}\right)^2 - \beta_2\left(\frac{\alpha_s}{4\pi}\right)^3 - \beta_3\left(\frac{\alpha_s}{4\pi}\right)^4 + \dots\,,\\
\gamma_m &= \frac{d\log m_q}{d\log\mu} = -\gamma_0\left(\frac{\alpha_s}{4\pi}\right) - \gamma_1\left(\frac{\alpha_s}{4\pi}\right)^2 - \gamma_2\left(\frac{\alpha_s}{4\pi}\right)^3 - \gamma_3\left(\frac{\alpha_s}{4\pi}\right)^4 \dots\,,
\end{aligned} \tag{108}$$

[23] In the notation of Ref. [39], where a different operator basis involving $J \equiv \sum_q \partial_\mu A_q^\mu$ was chosen, we have $Z_{5gq}^{(0)} = \left(Z_{G\tilde{G},\overline{\rm MS}}\right)^{-1} Z_{GJ,\overline{\rm MS}} Z_A^{\rm singlet}$ and $Z_{5gg}^{(0)} = \left(Z_{G\tilde{G},\overline{\rm MS}}\right)^{-1}\left[1 - \frac{g^2}{32\pi^2} n_f Z_{GJ,\overline{\rm MS}} Z_A^{\rm singlet}\right]$, where $Z_A^{\rm singlet}$ is given in (105) and $Z_{G\tilde{G},\overline{\rm MS}}$, $Z_{GJ,\overline{\rm MS}}$ are the quantities denoted by $Z_{G\tilde{G}}$, Z_{GJ} in Ref. [39].

where the ellipses denote terms higher order in α_s, and the required functions are

$$\begin{aligned}
\beta_0 &= 11 - \frac{2}{3}n_f\,, \\
\beta_1 &= 102 - \frac{38}{3}n_f\,, \\
\beta_2 &= \frac{2857}{2} - \frac{5033}{18}n_f + \frac{325}{54}n_f^2\,, \\
\beta_3 &= \frac{149753}{6} + 3564\zeta(3) - \left(\frac{1078361}{162} + \frac{6508}{27}\zeta(3)\right)n_f + \left(\frac{50065}{162} + \frac{6472}{81}\zeta(3)\right)n_f^2 + \frac{1093}{729}n_f^3\,, \quad (109)
\end{aligned}$$

and

$$\begin{aligned}
\gamma_0 &= 8\,, \\
\gamma_1 &= \frac{404}{3} - \frac{40}{9}n_f\,, \\
\gamma_2 &= 2498 - \left(\frac{4432}{27} + \frac{320}{3}\zeta(3)\right)n_f - \frac{280}{81}n_f^2\,, \\
\gamma_3 &= \frac{4603055}{81} + \frac{271360}{27}\zeta(3) - 17600\zeta(5) + \left(-\frac{183446}{27} - \frac{68384}{9}\zeta(3) + 1760\zeta(4) + \frac{36800}{9}\zeta(5)\right)n_f \\
&\quad + \left(\frac{10484}{243} + \frac{1600}{9}\zeta(3) - \frac{320}{3}\zeta(4)\right)n_f^2 + \left(-\frac{664}{243} + \frac{128}{27}\zeta(3)\right)n_f^3\,. \quad (110)
\end{aligned}$$

B Nucleon matrix elements

B.1 Corrections to zero momentum transfer

The corrections to zero momentum transfer are severely suppressed in the nonrelativistic regime of typical WIMP-nucleon scattering processes. To gauge the impact of these corrections in general models, we summarize current knowledge, identifying uncertainties that should be revisited if observables are found to be sensitive to these parameters.

The q^2 dependence of vector form factors may be investigated using the definition of the nucleon charge radii,

$$\left.\frac{d}{dq^2}F_1^{(N)}\right|_{q^2=0} \equiv \frac{1}{6}[r_E^{(N)}]^2 - \frac{a_N}{4m_N^2}\,, \quad (111)$$

with $[r_E^{(p)}]^2 = 0.70\,\mathrm{fm}^2 - 0.77\,\mathrm{fm}^2$ [94] and $[r_E^{(n)}]^2 = -0.1161(22)\,\mathrm{fm}^2$ [95].[24] Together with estimates for the numerically small strange contribution,

$$\left.\frac{d}{dq^2}F_1^{(p,s)}\right|_{q^2=0} \equiv \frac{1}{6}r_s^2\,, \quad r_s^2 = 0.021 \pm 0.063\,\mathrm{fm}^2 \text{ [96]}\,, \quad (112)$$

[24] This definition is motivated by considering the Sachs electric form factor $G_E(q^2) = F_1(q^2) + (q^2/m_N^2)F_2(q) \approx G_E(0) + \frac{1}{6}r_E^2 q^2 + \mathcal{O}(q^4)$. The proton charge radius is the subject of significant debate, but discrepancies are at a level of precision far beyond what is currently required for dark matter applications.

we may solve for the leading Taylor expansion of the quark vector current matrix elements,

$$\left.\frac{d}{dq^2}F_1^{(p,u)}\right|_{q^2=0} = 2\left(\frac{1}{6}[r_E^{(p)}]^2 - \frac{a_p}{4m_p^2}\right) + \left(\frac{1}{6}[r_E^{(n)}]^2 - \frac{a_n}{4m_n^2}\right) + \frac{1}{6}r_s^2\,,$$
$$\left.\frac{d}{dq^2}F_1^{(p,d)}\right|_{q^2=0} = \left(\frac{1}{6}[r_E^{(p)}]^2 - \frac{a_p}{4m_p^2}\right) + 2\left(\frac{1}{6}[r_E^{(n)}]^2 - \frac{a_n}{4m_n^2}\right) + \frac{1}{6}r_s^2\,. \tag{113}$$

Again, we approximate the neutron form factors by the corresponding proton form factors using approximate isospin symmetry expressed in (42).

The q^2 dependence of axial-vector form factors may be investigated, writing

$$F_A^{(p,a)}(q^2) = F_A^{(p,a)}(0)\left[1 + 2q^2/m_A^{(a)2} + \mathcal{O}(q^4)\right], \tag{114}$$

with $m_A^{(3)} \approx m_A^{(8)} \approx m_A^{(0)} \approx 1.0\,\mathrm{GeV}$ denoting an "axial mass" scale. There remains considerable uncertainty on the q^2 dependence of the isovector axial-vector form factor, with a conservative treatment of shape uncertainty yielding [97] $m_A^{(3)} = 0.85(22)(8)\,\mathrm{GeV}$ from neutrino scattering and $m_A^{(3)} = 0.92(13)(8)\,\mathrm{GeV}$ from pion electroproduction. The octet and flavor-singlet cases are less constrained. For definiteness we take also $m_A^{(8)} = m_A^{(0)} = 1.0(3)\,\mathrm{GeV}$ as default values, which should be revisited if observables are found to be sensitive to these parameters.

For the induced pseudoscalar form factors, the isovector component is best determined [98],

$$F_{P'}^{(p,3)}(q^2) = \frac{1}{2}\left[\frac{4m_p g_{\pi N} f_\pi}{m_\pi^2 - q^2} - \frac{2}{3}g_A m_p^2 r_A^2 + \mathcal{O}(q^2, m_\pi^2)\right], \tag{115}$$

with $f_\pi = 93\,\mathrm{MeV}$, m_π and m_p denoting the charged pion and proton masses respectively, $g_A = 1.267(4)$ the axial coupling constant, $g_{\pi N} = 13.1(4)$ the pion-nucleon coupling and $r_A^2/6 = 2/m_A^{(3)2}$ giving the slope of the form factor as in (114). In particular, in the chiral limit,

$$F_{P'}^{(p,3)}(0) \sim \frac{g_A}{2}\frac{4m_p^2}{m_\pi^2}\,, \tag{116}$$

diverging as $m_\pi \to 0$. For the octet contribution, a similar enhancement behaving as m_p^2/m_η^2 emerges,

$$F_{P'}^{(p,8)}(0) \sim \frac{2m_p^2}{m_\eta^2}\,. \tag{117}$$

while for the flavor singlet case the absence of a pseudo Nambu Goldstone boson coupling to the current implies the absence of such an enhancement,

$$F_{P'}^{(p,0)}(0) \sim \mathcal{O}(1)\,. \tag{118}$$

Large $SU(3)$ breaking corrections modify relations such as (117), which should be accounted for by allowing significant variation in the assumed form factors.

B.2 Heavy quark scalar matrix elements

The $\mathcal{O}(\alpha_s^3)$ term in (39) is given by

$$\langle O_Q'^{(0)}\rangle_4 = \frac{6628017}{8}\log^2\frac{\mu_Q}{m_Q} + \frac{3325355}{8}\log\frac{\mu_Q}{m_Q} - \frac{37326201}{8}\lambda\log^2\frac{\mu_Q}{m_Q} - \frac{32191115}{8}\lambda\log\frac{\mu_Q}{m_Q}$$

$$
- \frac{2387203071\zeta(3)}{512}\lambda + \frac{3852721945}{768}\lambda + \frac{3399188991\zeta(3)}{512} - \frac{6064085209}{768}
$$

$$
+ n_f\Bigg\{ 25234\log^2\frac{\mu_Q}{m_Q} - \frac{244697}{8}\log\frac{\mu_Q}{m_Q} + 1167584\lambda\log^2\frac{\mu_Q}{m_Q} + \frac{6596273}{8}\lambda\log\frac{\mu_Q}{m_Q}
$$

$$
+ \frac{181905471\zeta(3)}{128}\lambda - \frac{36859013}{32}\lambda - \frac{227904831\zeta(3)}{128} + \frac{195412223}{96}\Bigg\}
$$

$$
n_f^2\Bigg\{ - \frac{116243}{3}\log^2\frac{\mu_Q}{m_Q} + \frac{433163}{48}\log\frac{\mu_Q}{m_Q} - \frac{328597}{3}\lambda\log^2\frac{\mu_Q}{m_Q} - \frac{3504107}{48}\lambda\log\frac{\mu_Q}{m_Q}
$$

$$
- 147631\lambda\zeta(3) + \frac{51820165}{576}\lambda + 169411\zeta(3) - \frac{120231661}{576}\Bigg\}
$$

$$
n_f^3\Bigg\{ \frac{41840}{9}\log^2\frac{\mu_Q}{m_Q} - \frac{340895}{216}\log\frac{\mu_Q}{m_Q} + \frac{13696}{3}\lambda\log^2\frac{\mu_Q}{m_Q} + \frac{820223}{216}\lambda\log\frac{\mu_Q}{m_Q}
$$

$$
+ \frac{1839305\zeta(3)}{288}\lambda - \frac{1088479}{324}\lambda - \frac{1966025\zeta(3)}{288} + \frac{3637345}{324}\Bigg\}
$$

$$
n_f^4\Bigg\{ - \frac{1934}{9}\log^2\frac{\mu_Q}{m_Q} + \frac{9421}{108}\log\frac{\mu_Q}{m_Q} - \frac{214}{3}\lambda\log^2\frac{\mu_Q}{m_Q} - \frac{12397}{108}\lambda\log\frac{\mu_Q}{m_Q} - \frac{28297\zeta(3)}{288}\lambda
$$

$$
+ \frac{7519}{162}\lambda + \frac{28297\zeta(3)}{288} - \frac{886}{3}\Bigg\}
$$

$$
+ n_f^5\Bigg\{ \frac{32}{9}\log^2\frac{\mu_Q}{m_Q} - \frac{77}{54}\log\frac{\mu_Q}{m_Q} + \frac{77}{54}\lambda\log\frac{\mu_Q}{m_Q} + \frac{5}{54}\lambda + \frac{481}{162}\Bigg\}, \tag{119}
$$

where m_Q is the $\overline{\rm MS}$ quark mass. Scheme dependence enters at this order and we have checked that the result in terms of the pole mass, employing the relevant functions in Ref. [51], is consistent with the relation between $\overline{\rm MS}$ and pole masses given in Ref. [53]. This result is employed in the determination of the charm quark matrix element in (61) which, in terms of an α_s expansion, is given by

$$
\tilde{f}_{c,N}^{(0)} = 0.074(1-\lambda) + \frac{\alpha^{(4)}(\mu_c)}{\pi}\Bigg\{0.072 - 0.220\lambda\Bigg\} + \left(\frac{\alpha^{(4)}(\mu_c)}{\pi}\right)^2\Bigg\{0.100 - 0.528\lambda
$$

$$
+ [0.300 - 0.917\lambda]\log\frac{\mu_c}{m_c}\Bigg\} + \left(\frac{\alpha^{(4)}(\mu_c)}{\pi}\right)^3\Bigg\{ - 0.391 + 0.761\lambda
$$

$$
+ [0.694778 - 3.977\lambda]\log\frac{\mu_c}{m_c} + [1.25029 - 3.8223\lambda]\log^2\frac{\mu_c}{m_c}\Bigg\} + \mathcal{O}(\alpha_s^4)\,. \tag{120}
$$

References

[1] P. Cushman, C. Galbiati, D. N. McKinsey, H. Robertson, T. M. P. Tait, D. Bauer, A. Borgland and B. Cabrera *et al.*, "Working Group Report: WIMP Dark Matter Direct Detection," arXiv:1310.8327 [hep-ex].

[2] G. Buchalla, A. J. Buras and M. E. Lautenbacher, Rev. Mod. Phys. **68**, 1125 (1996) [hep-ph/9512380].

[3] J. Engel, M. J. Ramsey-Musolf and U. van Kolck, Prog. Part. Nucl. Phys. **71**, 21 (2013) [arXiv:1303.2371 [nucl-th]].

[4] R. J. Hill and M. P. Solon, arXiv:1401.3339 [hep-ph].

[5] G. Jungman, M. Kamionkowski and K. Griest, Phys. Rept. **267**, 195 (1996) [arXiv:hep-ph/9506380].

[6] J. L. Feng, Ann. Rev. Nucl. Part. Sci. **63**, 351 (2013) [arXiv:1302.6587 [hep-ph]].

[7] A. Fowlie *et al.* [BayesFITS Group Collaboration], Phys. Rev. D **88**, no. 5, 055012 (2013) [arXiv:1306.1567 [hep-ph]].

[8] S. Chang, R. Edezhath, J. Hutchinson and M. Luty, Phys. Rev. D **89**, 015011 (2014) [arXiv:1307.8120 [hep-ph]].

[9] H. An, L. T. Wang and H. Zhang, Phys. Rev. D **89**, 115014 (2014) [arXiv:1308.0592 [hep-ph]].

[10] Y. Bai and J. Berger, JHEP **1311**, 171 (2013) [arXiv:1308.0612 [hep-ph]].

[11] A. DiFranzo, K. I. Nagao, A. Rajaraman and T. M. P. Tait, JHEP **1311**, 014 (2013) [arXiv:1308.2679 [hep-ph]].

[12] Y. Bai and J. Berger, JHEP **1408**, 153 (2014) [arXiv:1402.6696 [hep-ph]].

[13] S. Chang, R. Edezhath, J. Hutchinson and M. Luty, Phys. Rev. D **90**, 015011 (2014) [arXiv:1402.7358 [hep-ph]].

[14] P. Agrawal, Z. Chacko and C. B. Verhaaren, JHEP **1408**, 147 (2014) [arXiv:1402.7369 [hep-ph]].

[15] R. J. Hill and M. P. Solon, Phys. Lett. B **707**, 539 (2012) [arXiv:1111.0016 [hep-ph]].

[16] R. J. Hill and M. P. Solon, Phys. Rev. Lett. **112**, 211602 (2014) [arXiv:1309.4092 [hep-ph]].

[17] J. Goodman, M. Ibe, A. Rajaraman, W. Shepherd, T. M. P. Tait and H. -B. Yu, Phys. Rev. D **82**, 116010 (2010) [arXiv:1008.1783 [hep-ph]].

[18] S. Matsumoto, S. Mukhopadhyay and Y. -L. S. Tsai, arXiv:1407.1859 [hep-ph].

[19] A. Crivellin, F. D'Eramo and M. Procura, Phys. Rev. Lett. **112**, 191304 (2014) [arXiv:1402.1173 [hep-ph]].

[20] A. Crivellin and U. Haisch, arXiv:1408.5046 [hep-ph].

[21] A. L. Fitzpatrick, W. Haxton, E. Katz, N. Lubbers and Y. Xu, JCAP **1302**, 004 (2013) [arXiv:1203.3542 [hep-ph]].

[22] A. L. Fitzpatrick, W. Haxton, E. Katz, N. Lubbers and Y. Xu, arXiv:1211.2818 [hep-ph].

[23] N. Anand, A. L. Fitzpatrick and W. C. Haxton, Phys. Rev. C **89**, 065501 (2014) [arXiv:1308.6288 [hep-ph]].

[24] R. Catena and P. Gondolo, arXiv:1405.2637 [hep-ph].

[25] M. W. Goodman and E. Witten, Phys. Rev. D **31**, 3059 (1985).

[26] V. Cirigliano, M. L. Graesser and G. Ovanesyan, JHEP **1210**, 025 (2012) [arXiv:1205.2695 [hep-ph]].

[27] J. Fan, M. Reece and L. -T. Wang, JCAP **1011**, 042 (2010) [arXiv:1008.1591 [hep-ph]].

[28] A. H. G. Peter, V. Gluscevic, A. M. Green, B. J. Kavanagh and S. K. Lee, arXiv:1310.7039 [astro-ph.CO].

[29] J. Menendez, D. Gazit and A. Schwenk, Phys. Rev. D **86**, 103511 (2012) [arXiv:1208.1094 [astro-ph.CO]].

[30] P. Klos, J. Menndez, D. Gazit and A. Schwenk, Phys. Rev. D **88**, 083516 (2013) [arXiv:1304.7684 [nucl-th]].

[31] S. Gardner and G. Fuller, Prog. Part. Nucl. Phys. **71**, 167 (2013) [arXiv:1303.4758 [hep-ph]].

[32] M. Cirelli, E. Del Nobile and P. Panci, JCAP **1310**, 019 (2013) [arXiv:1307.5955 [hep-ph]].

[33] J. Heinonen, R. J. Hill and M. P. Solon, Phys. Rev. D **86**, 094020 (2012) [arXiv:1208.0601 [hep-ph]].

[34] K. Kopp and T. Okui, Phys. Rev. D **84**, 093007 (2011) [arXiv:1108.2702 [hep-ph]].

[35] M. E. Luke and A. V. Manohar, Phys. Lett. B **286**, 348 (1992) [hep-ph/9205228]. A. V. Manohar, Phys. Rev. D **56**, 230 (1997) [hep-ph/9701294]. N. Brambilla, D. Gromes and A. Vairo, Phys. Lett. B **576**, 314 (2003) [hep-ph/0306107].

[36] R. J. Hill, G. Lee, G. Paz and M. P. Solon, Phys. Rev. D **87**, 053017 (2013) [arXiv:1212.4508 [hep-ph]].

[37] M. A. Fedderke, J. Y. Chen, E. W. Kolb and L. T. Wang, JHEP **1408**, 122 (2014) [arXiv:1404.2283 [hep-ph]].

[38] M. Freytsis and Z. Ligeti, Phys. Rev. D **83**, 115009 (2011) [arXiv:1012.5317 [hep-ph]].

[39] S. A. Larin, Phys. Lett. B **303**, 113 (1993) [hep-ph/9302240], and references therein.

[40] S. Kumano and M. Miyama, Phys. Rev. D **56**, 2504 (1997) [hep-ph/9706420].

[41] A. Hayashigaki, Y. Kanazawa and Y. Koike, Phys. Rev. D **56**, 7350 (1997) [hep-ph/9707208].

[42] W. Vogelsang, Phys. Rev. D **57**, 1886 (1998) [hep-ph/9706511].

[43] A. Vogt, S. Moch and J. A. M. Vermaseren, Nucl. Phys. B **691**, 129 (2004) [hep-ph/0404111].

[44] S. Moch, J. A. M. Vermaseren and A. Vogt, Nucl. Phys. B **688**, 101 (2004) [hep-ph/0403192].

[45] R. Mertig and W. L. van Neerven, Z. Phys. C **70**, 637 (1996) [hep-ph/9506451].

[46] G. Prezeau, A. Kurylov, M. Kamionkowski and P. Vogel, Phys. Rev. Lett. **91**, 231301 (2003) [astro-ph/0309115].

[47] S. R. Beane, S. D. Cohen, W. Detmold, H.-W. Lin and M. J. Savage, Phys. Rev. D **89**, 074505 (2014) [arXiv:1306.6939 [hep-ph]].

[48] A. G. Grozin, Phys. Lett. B **445**, 165 (1998) [hep-ph/9810358].

[49] A. G. Grozin, A. V. Smirnov and V. A. Smirnov, JHEP **0611**, 022 (2006) [hep-ph/0609280].

[50] T. Inami, T. Kubota and Y. Okada, Z. Phys. C **18**, 69 (1983).

[51] K. G. Chetyrkin, B. A. Kniehl and M. Steinhauser, Nucl. Phys. B **510**, 61 (1998) [hep-ph/9708255].

[52] A. G. Grozin, M. Hoeschele, J. Hoff, M. Steinhauser, M. Hoschele, J. Hoff and M. Steinhauser, JHEP **1109**, 066 (2011) [arXiv:1107.5970 [hep-ph]].

[53] K. G. Chetyrkin, J. H. Kuhn and M. Steinhauser, Comput. Phys. Commun. **133**, 43 (2000) [hep-ph/0004189].

[54] L. Vecchi, arXiv:1312.5695 [hep-ph].

[55] A. Kryjevski, Phys. Rev. D **70**, 094028 (2004) [hep-ph/0312196].

[56] D. B. Leinweber, S. Boinepalli, I. C. Cloet, A. W. Thomas, A. G. Williams, R. D. Young, J. M. Zanotti and J. B. Zhang, Phys. Rev. Lett. **94**, 212001 (2005) [hep-lat/0406002].

[57] T. Doi, M. Deka, S. -J. Dong, T. Draper, K. -F. Liu, D. Mankame, N. Mathur and T. Streuer, Phys. Rev. D **80**, 094503 (2009) [arXiv:0903.3232 [hep-ph]].

[58] For recent reviews see: D. S. Armstrong and R. D. McKeown, Ann. Rev. Nucl. Part. Sci. **62**, 337 (2012) [arXiv:1207.5238 [nucl-ex]]. R. Gonzalez-Jimenez, J. A. Caballero and T. W. Donnelly, Phys. Rept. **524**, 1 (2013) [arXiv:1111.6918 [nucl-th]].

[59] D. B. Kaplan and A. Manohar, Nucl. Phys. B **310**, 527 (1988).

[60] E. R. Nocera *et al.* [The NNPDF Collaboration], arXiv:1406.5539 [hep-ph].

[61] M. Fukugita, Y. Kuramashi, M. Okawa and A. Ukawa, Phys. Rev. Lett. **75**, 2092 (1995) [hep-lat/9501010].

[62] S. J. Dong and K. F. Liu, Nucl. Phys. Proc. Suppl. **42**, 322 (1995) [hep-lat/9412059].

[63] S. Aoki, M. Doui, T. Hatsuda and Y. Kuramashi, Phys. Rev. D **56**, 433 (1997) [hep-lat/9608115].

[64] D. Dolgov *et al.* [LHPC and TXL Collaborations], Phys. Rev. D **66**, 034506 (2002) [hep-lat/0201021].

[65] M. Gockeler *et al.* [QCDSF and UKQCD Collaborations], Phys. Lett. B **627**, 113 (2005) [hep-lat/0507001].

[66] H. W. Lin, T. Blum, S. Ohta, S. Sasaki and T. Yamazaki, Phys. Rev. D **78**, 014505 (2008) [arXiv:0802.0863 [hep-lat]].

[67] H. x. He and X. D. Ji, Phys. Rev. D **52**, 2960 (1995) [hep-ph/9412235].

[68] M. Wakamatsu, Phys. Lett. B **653**, 398 (2007) [arXiv:0705.2917 [hep-ph]].

[69] I. C. Cloet, W. Bentz and A. W. Thomas, Phys. Lett. B **659**, 214 (2008) [arXiv:0708.3246 [hep-ph]].

[70] M. Anselmino, M. Boglione, U. D'Alesio, A. Kotzinian, F. Murgia, A. Prokudin and S. Melis, Nucl. Phys. Proc. Suppl. **191**, 98 (2009) [arXiv:0812.4366 [hep-ph]].

[71] J. Beringer *et al.* [Particle Data Group Collaboration], Phys. Rev. D **86**, 010001 (2012).

[72] Z. z. Xing, H. Zhang and S. Zhou, Phys. Rev. D **77**, 113016 (2008) [arXiv:0712.1419 [hep-ph]].

[73] J. Gasser and H. Leutwyler, Phys. Rept. **87**, 77 (1982).

[74] S. Durr, Z. Fodor, T. Hemmert, C. Hoelbling, J. Frison, S. D. Katz, S. Krieg and T. Kurth *et al.*, Phys. Rev. D **85**, 014509 (2012).

[75] P. Junnarkar and A. Walker-Loud, Phys. Rev. D **87**, 114510 (2013).

[76] A. Crivellin, M. Hoferichter and M. Procura, Phys. Rev. D **89**, 054021 (2014) [arXiv:1312.4951 [hep-ph]].

[77] W. Freeman *et al.* [MILC Collaboration], Phys. Rev. D **88**, 054503 (2013).

[78] M. Gong, A. Alexandru, Y. Chen, T. Doi, S. J. Dong, T. Draper, W. Freeman and M. Glatzmaier *et al.*, Phys. Rev. D 88, **014503** (2013).

[79] H. Y. Cheng and C. W. Chiang, JHEP **1207**, 009 (2012) [arXiv:1202.1292 [hep-ph]].

[80] A. D. Martin, W. J. Stirling, R. S. Thorne and G. Watt, Eur. Phys. J. C **63**, 189 (2009) [arXiv:0901.0002 [hep-ph]].

[81] J. Kodaira and K. Tanaka, Prog. Theor. Phys. **101**, 191 (1999) [hep-ph/9812449].

[82] N. Brambilla, E. Mereghetti and A. Vairo, Phys. Rev. D **79**, 074002 (2009) [Erratum-ibid. D **83**, 079904 (2011)] [arXiv:0810.2259 [hep-ph]].

[83] J. L. Feng, J. Kumar, D. Marfatia and D. Sanford, Phys. Lett. B **703**, 124 (2011) [arXiv:1102.4331 [hep-ph]].

[84] J. Hisano, K. Ishiwata, N. Nagata, T. Takesako, JHEP **1107**, 005 (2011). [arXiv:1104.0228 [hep-ph]]. J. Hisano, K. Ishiwata and N. Nagata, Phys. Rev. D **87**, 035020 (2013) [arXiv:1210.5985 [hep-ph]].

[85] M. A. Shifman, A. I. Vainshtein and V. I. Zakharov, Phys. Lett. B **78**, 443 (1978).

[86] U. Haisch and F. Kahlhoefer, JCAP **1304**, 050 (2013) [arXiv:1302.4454 [hep-ph]].

[87] J. R. Ellis, J. S. Lee and A. Pilaftsis, JHEP **0810**, 049 (2008) [arXiv:0808.1819 [hep-ph]].

[88] C. Adams *et al.* [LBNE Collaboration], arXiv:1307.7335 [hep-ex].

[89] T. Miceli *et al.* [MicroBooNE Collaboration], arXiv:1406.5204 [hep-ex].

[90] J. R. Ellis, K. A. Olive and C. Savage, Phys. Rev. D **77**, 065026 (2008) [arXiv:0801.3656 [hep-ph]].

[91] M. Beltran, D. Hooper, E. W. Kolb, Z. A. C. Krusberg and T. M. P. Tait, JHEP **1009**, 037 (2010) [arXiv:1002.4137 [hep-ph]].

[92] E. Aprile *et al.* [XENON100 Collaboration], Phys. Rev. Lett. **109**, 181301 (2012) [arXiv:1207.5988 [astro-ph.CO]].

[93] D. S. Akerib *et al.* [LUX Collaboration], Phys. Rev. Lett. **112**, 091303 (2014) [arXiv:1310.8214 [astro-ph.CO]].

[94] P. J. Mohr, B. N. Taylor and D. B. Newell, Rev. Mod. Phys. **84**, 1527 (2012) [arXiv:1203.5425 [physics.atom-ph]].

[95] K. Nakamura *et al.* [Particle Data Group Collaboration], J. Phys. G **37**, 075021 (2010).

[96] D. B. Leinweber, S. Boinepalli, A. W. Thomas, P. Wang, A. G. Williams, R. D. Young, J. M. Zanotti and J. B. Zhang, Phys. Rev. Lett. **97**, 022001 (2006) [hep-lat/0601025].

[97] B. Bhattacharya, R. J. Hill and G. Paz, Phys. Rev. D **84**, 073006 (2011) [arXiv:1108.0423 [hep-ph]].

[98] V. Bernard, L. Elouadrhiri and U. .G. Meissner, J. Phys. G **28**, R1 (2002) [hep-ph/0107088].